Environmental
Studies
Research
Funds

125

Long-Range Ice Forecasting System (LRIFS)

Applied for the Beaufort Sea

Canada

March 1991

The Environmental Studies Research Funds are financed from special levies on the oil and gas industry and are administered by the National Energy Board for the Minister of Energy, Mines and Resources, and for the Minister of Indian Affairs and Northern Development.

Environmental Studies Research Funds

Report No. 125

May 1993

Long-Range Ice Forecasting System (LRIFS) Applied for the Beaufort Sea

L.W. Davidson, M. Sc.
Seaconsult Limited
200 White Hills Road
P.O. Box 2035, Station C
St. John's NF
A1C 5R6

Scientific Advisor: Oleh Mycyk

The correct citation for this report is:

Davidson, L.W., 1993. Long-Range Ice Forecasting System (LRIFS) Applied for the Beaufort Sea. Environmental Studies Research Funds, Report No. 125. Calgary, Alberta.

Published under the auspices of the Environmental Studies Research Funds

ISBN 0-921652-27-5

Table of Contents

List of Tables

List of Figures

List of Acronyms, Symbols, and Abbreviations

A	Ice Area Index (also ICEA)
a(n)	Eigenfunction Coefficient (also a_n)
AES	Atmospheric Environment Service
CMC	Canadian Meteorological Centre
CSI	Composite Skill Index
D500	1000 - 500 mb Thickness
D700	1000 - 700 mb Thickness
E(n)	Eigenfunction or Eigenvector (also E_n)
EOF	Empirical Orthogonal Function
ESRF	Environmental Studies Research Funds
H1000	1000 mb Geopotential Height
H500	500 mb Geopotential Height
H700	700 mb Geopotential Height
ICEA	Ice Area Index (also A)
ICEC	Ice Centre Environment Canada
IIP	International Ice Patrol
LRIFS	Long Range Ice Forecasting System
m	Number of important eigenvectors
M	Number of time intervals
MSLP	Mean Sea Level Pressure
N1	Number of columns in predictor data grid
N2	Number of rows in predictor data grid
NASA	National Aeronautics and Space Administration
NCAR	National Centre for Atmospheric Research
NMC	National Meteorological Centre
P(x,y,t)	Zero-mean scalar anomaly field
R^2	Coefficient of Determination
r	Correlation Coefficient
R_{ij}	Time averaged correlation matrix of anomaly fields
SAT	Surface Air Temperature
SLP	Sea Level Pressure
SST	Sea Surface Temperature
$\bar{x}$	Mean
x,y	Spatial Coordinates
$\underline{x}$	Spatial Coordinate
$\lambda(n)$	Eigenvalue (also λ_n)
σ	Standard Deviation

Acknowledgements

The current work follows from earlier investigations of statistical forecasting techniques for the long-range prediction of iceberg and sea ice season severity on the Canadian east coast. The author remains indebted to Mr. Oleh Mycyk of the National Energy Board for his motivation in initiating the earliest east coast work, and for his decade of consistent technical and managerial support of subsequent research, culminating in the present Beaufort Sea investigations. Paralleling the support of Mr. Mycyk and his colleagues at the National Energy Board has been consistent cooperation and support from Ice Centre Environment Canada, directed by Mr. Tom Carrieres, and benefiting also from the attention of Mr. Terry Mullane and Mr. Laurent Chenard.

Sincere appreciation is expressed by the author directly to his associates at Seaconsult Limited who have made significant technical contributions to this and previous related research. Most particularly the work of Mr. Jeff Pinhorn and Mr. Terry Lomax is to be commended. Our associate Dr. John Walsh at the University of Illinois is recognized as an important contributor to this work, through his frequent suggestions, offered usually at times of technical difficulty, and delivered always with the utmost consideration.

Executive Summary

Applied research conducted from 1984 to 1990 on behalf of the Environmental Studies Research Funds (ESRF) and Ice Centre Environment Canada (ICEC) has resulted in the implementation of an operational Long Range Ice (sea ice and iceberg severity) Forecasting System (LRIFS) at Ice Centre, Ottawa. The LRIFS system employs statistical models based on Empirical Orthogonal Function (EOF) analyses of up to 40 years of regional surface and upper air weather data to predict abundance of sea ice and icebergs, in some locations up to six months prior to occurrence. The system also makes provision of the use of ice anomaly data to predict future ice conditions. In the present work, this system has been generalized from its previous east coast base, and is now configured for use anywhere in the northern hemisphere. Major enhancements have been introduced to automate the identification of potentially viable meteorological predictors, and tests have been added to eliminate predictors showing artificial skill.

The LRIFS system has been applied to develop operational long range forecast equations for sea ice area in the Beaufort Sea. Results presented here indicate that forecast lead times of a few months which appear to have been achieved for the east coast are not achievable for the Beaufort Sea. Operational equations are derived at best for one month lead times in July, August, and September, and for the three month interval July through September. These are shown in most instances to depend heavily on sea ice anomaly persistence as one of the predictors in the multiple regression forecast models. Nevertheless, for these relatively short lead time models, correlation coefficients calculated between predicted and observed ice area routinely achieve values well in excess of 90%. A major impediment to the application of LRIFS for Beaufort Sea use is the very short (1960 to 1980) interval of digital sea ice data which is available. This fact leads to the primary recommendation of the work, which is that the predictand data base be extended to include the interval 1981 through 1992.

RÉSUMÉ

La recherche appliquée, menée de 1984 à 1990 pour le Fonds pour l'étude de l'environnement et le Centre des glaces d'Environnement Canada a abouti à la mise d'un système de prévision à longue portée des glaces (glaces de mer et icebergs) au Centre des glaces, à Ottawa. Des modèles statistiques, basés sur les analyses de la fonction orthogonale empirique de plus de 40 ans de données sur les conditions régionales en surface et en altitude, servent à prédire l'abondance des glaces de mer et des icebergs, jusqu'à six mois à l'avance à certains endroits. Les données sur les anomalies des glaces sont aussi utilisées pour prédire le futur régime des glaces. Le système s'appliquait seulement à la côte est, mais il a été généralisé et sa configuration actuelle en permet l'utilisation partout dans l'hémisphère nord. Au nombre des grandes améliorations apportées, l'identification des prédicteurs viables a été automatisée et des tests ont été ajoutés pour éliminer les prédicteurs montrant une capacité artificielle.

Le système a servi à développer des équations opérationnelles de prévision à longue portée sur l'étendue de glaces dans la mer de Beaufort. Selon les résultats ici présentés, les délais de prévision de quelques mois qui semblent avoir été obtenus pour la côte est ne sont pas réalisables pour la mer de Beaufort. Les équations opérationnelles visent au mieux un mois en juillet, août et septembre, et trois mois de juillet à septembre. Dans la plupart des cas, elles dépendent fortement de la persistance des anomalies comme l'un des prédicteurs des modèles de régression multiple. Néanmoins, pour des délais relativement courts, les coefficients de corrélation entre l'étendue prévue et l'étendue réelle calculés permettent couramment d'obtenir des valeurs supérieures à 90 %. L'intervalle très court (de 1960 à 1980) des données numériques sur les glaces de mer qui est disponible constitue un gros obstacle à la mise en oeuvre du système en ce qui a trait à la mer de Beaufort. Il est donc avant tout recommander d'élargir la base de données des prédicants pour comprendre l'intervalle entre 1981 et 1992.

1. INTRODUCTION AND PURPOSE

1.1 Setting

Statistical models based on Empirical Orthogonal Function (EOF) analyses of up to 40 years of regional surface and upper air weather data have been installed operationally since 1991 in the Long Range Ice Forecasting System (LRIFS) at Ice Centre Environment Canada, in Ottawa. Theses models are employed to predict the abundance of sea ice and icebergs on the Canadian east coast, up to six months prior to occurrence. This report describes work undertaken under funding from the Environmental Studies Research Funds (ESRF), by Seaconsult Limited of St. John's, Newfoundland, to investigate whether these same or similar methods can successfully be applied to predict Beaufort Sea sea ice abundance and timing, in advance of the ice season. This work has been partially supported by Environment Canada, and has been conducted under the joint technical project management of Mr. Oleh Mycyk, representing the interests of ESRF, and Mr. Tom Carrieres, representing the interests of Ice Centre, Environment Canada.

1.2 Previous Research

At the height of early 1980's hydrocarbon exploration activity on the Grand Banks, funding was made available through the Environmental Studies Research Funds (ESRF) to attempt the long-range prediction of Grand Banks iceberg season severity. The term "long-range" here refers to the issue of forecasts one to several months in advance of the predicted event. Two independent studies commenced in 1984 with ESRF support. One, reported by Marko et al. (1986), attempted the use of deterministic methods based on physical transport mechanisms to predict iceberg abundance. This work did not result in the development of an operational model for long-range severity prediction. The other, reported by Davidson et al. (1986), employed statistical methods based on regional fields of meteorological parameters, again to predict annual iceberg abundance south of 48° N latitude. Although this work did not yield an operational long-range severity prediction model, its methods were employed to accurately predict the severity of the 1986 Grand Banks iceberg season. Based on 30 year hindcast tests (1951-1980), models developed in this study were highly successful in predicting the most severe years. Some 27 of 30 years were predicted with moderate to good accuracy.

An attempted extension of the statistical prediction approach is reported by Davidson (1987). The use of sea surface temperature (SST) data as an additional predictor field was investigated and determined to be premature, based on the conclusion that "available collections of SST data are far too sparse in the more northerly regions, to justify their use in statistical schemes for long-range iceberg season severity prediction". As well, analogue-assisted forecasting for late season predictors was investigated, but was found to yield only fractional, if any, improvements in forecast skill over the direct use of earlier season predictors.

In a major extension of this iceberg severity prediction work between 1989 and 1992, the same statistical methods were implemented to attempt prediction of east coast sea ice severity. It was hypothesized that a transformed version of the iceberg severity prediction techniques would prove skilful in sea ice severity prediction. It was recognized that the sea ice problem is much more complex due to the spatial nature of sea ice distribution (versus the scalar nature of iceberg

flux), and due to the more rapid time scales of variability of sea ice distributions than of iceberg flux. Specific tasks included (i) investigation of indexing schemes for sea ice severity classification, and choice of schemes suitable for Canadian East Coast conditions; (ii) application of EOF techniques developed for iceberg season prediction, and selection of prospective predictors for east coast ice abundance in four distinct regions including the Gulf of St. Lawrence, the southeastern Grand Banks, the south/central Labrador Shelf, and the north Labrador shelf; (iii) isolation of predictors which are most skilful; and (iv) development of these into an operational long-range sea ice severity prediction scheme. This work, reported by Davidson (1992) resulted in the installation of the operational LRIFS system at Ice Centre Environment Canada.

Of particular interest to the present study is the history of long range ice severity prediction in the western Arctic. Research in long-range forecasting of Arctic sea ice has been active since the late 1970's, but progress has been slow (Chapman and Walsh, 1991). Early work on long-range forecasting of Arctic ice was undertaken by Barnett (1980), who discovered correlations between summer ice severity on the North Coast of Alaska and April meteorological conditions in Siberia.

Walsh (1980) studied the predictability of Arctic sea ice extent using empirical orthogonal functions. He found that for lags of up to one month, ice anomaly persistence (i.e. autocorrelation with previous sea ice conditions) proved to be the most skillful predictor. For lags of 1-2 months, predictors derived from meteorological fields were found to be nominally significant. For longer forecast lags, little significant skill was obtained.

Johnson, Lemke, and Barnett (1985) systematically investigated the prediction of Arctic sea ice anomalies using internal (i.e. sea ice) and external (i.e. atmospheric and oceanic) predictors with lags of up to 6 months. The highest skill was obtained using a cyclostationary internal model for lags of up to 2 months. The use of external predictors gave smaller skill with one exception: with a 3 month forecast lag, North Pacific SST was found to be a better predictor of ice in the western Bering Sea than lagged sea ice.

Chapman and Walsh (1991) compared an analog method of predicting Arctic sea ice anomalies with predictions using ice anomaly persistence. They report that while they show statistically significant skill, analog forecasts are unable to outperform simple persistence at lags of up to one month. Longer-range predictions were less successful, although lagged regional ice cross-correlations showed some promise.

Seasonal and interannual patterns in Arctic sea ice anomalies have also been reported (Barnett, 1980; Hibler and Walsh 1982; Mysak and Manak, 1989). In the Beaufort Sea, a 4-6 year cycle has been identified (Barnett, 1980; Mysak and Manak, 1989).

1.3 Scope and Purpose of Current Work

The following specific objectives were established for the current work.

- Develop Work Plan, Schedule, and Payment Plan

  Due to the combined financing of ESRF and Environment Canada, there was requirement for subdivision of technical tasks and financial/contractual obligations. The required Work Plan, Schedule, and Payment Plan was jointly submitted to ESRF and Environment Canada in January 1992. This technical report incorporates all pertinent technical information, whether applicable to the ESRF or to the Environment Canada portions of the work.

- Generalize to Hemispheric Predictor Data Files

  It was recognized as imperative that any system developed for Beaufort Sea operation be fully compatible with the existing East Coast LRIFS system. When this work commenced, that existing system operated on a fixed 15 x 15 element geographical grid of historical meteorological data (also referred to as predictor data). The desired approach was to generalize the handling of meteorological data so as to make predictor data from a much larger region (most probably the entire northern hemisphere), accessible to the long-range forecasting system for the purpose of searching for viable ice predictors. This generalized, hemispheric system would function identically for the East Coast, the Beaufort Sea, or for any other region.

- Prepare Predictor Data

  The necessary hemispheric weather files were to be prepared by extracting files of weather data from available sources onto the hemispheric predictor data grid. Data types (parameters) to be included in this extraction process were: (a) mean sea level pressure, (b) 1000 mb, 700 mb and 500 mb geopotential height, (c) 700-1000 mb and 500-1000 mb thickness, and (d) surface air temperature. The duration of weather data to be extracted was to more than exceed the duration of available Beaufort Sea sea ice occurrence data.

- Prepare Predictand Data

  Full years (ice seasons) of digital Beaufort Sea sea ice occurrence and distribution data were to be extracted from AES Ice Centre archives, for as long a continuous interval as possible.

- Automate Execution of Single/Multiple Regression Tests

  The past practice in selecting viable predictors had been to (i) manually prepare large numbers of execution commands for input to the linear regression package, causing large

numbers of linear regression tests to be run; (ii) visually assess the results of the linear regression test; (iii) manually prepare selected execution commands for the multiple regression package; and (iv) visually assess the results of the multiple regression tests to select most skilful equations. It was the purpose of this task to automate the first three of these four steps.

- Develop Forecast Equations for Beaufort Sea Sea Ice Occurrence

- Report Findings to ESRF and Ice Centre Environment Canada.

1.4 Complimentary Documents

It is important that the reader of this Technical Report recognize the relationship of this document to previously reported research as well as to other documents delivered to Ice Centre under this contract. This Technical Report deals almost exclusively with the scientific aspects of developing enhanced prediction schemes, identifying predictors, assessing forecast skill, modifying the LRIFS system, etc. One brief section (Chapter 4.6) quotes the specific prediction equations which have been recommended for installation in the operational forecast system at Ice Centre. With that exception, this report does not deal extensively with the operational forecast system. Rather, that system is detailed in two complimentary documents which have been delivered to Ice Centre. These are the System Specification referenced as Pinhorn (1993a) and the User's Manual referenced as Pinhorn (1993b). Neither does this report extensively revisit the evolution of the EOF forecasting methods. That history is well traced in the series of documents referenced as Davidson et al. (1986), Davidson (1987) and Davidson (1992).

2. LRIFS SYSTEM DESCRIPTION AND MODIFICATIONS

2.1 Review of Statistical Methods

The previous research discussed in Chapter 1.2 above was based on time-lagged correlation analyses between atmospheric features and ice severity indices for east coast sea ice and icebergs. The statistical method of Empirical Orthogonal Function (EOF) analysis was employed to extract dominant mode pattern information from long time-series (>30 years) of regional fields of atmospheric pressure, height, thickness and temperature data. Regression analyses were performed between coefficients describing the contribution of each such dominant mode to a particular monthly or seasonal data field, and various ice abundance indices. Thereby, it was possible to identify meteorological conditions early in the iceberg season (November to March), which were well correlated with iceberg abundance through the peak of the season (March to June). Multiple regression tests with groups of individually skilful predictors were then employed to identify practical multi-predictor forecast schemes. A synopsis of the relevant empirical orthogonal function (or eigenfunction) theory is reproduced from Davidson et al. (1986) as Appendix I. In practical terms, this method provides the means to test the correlation between ice severity indices in a particular location and season, and previous regional weather conditions.

2.2 Methods for Assessing Forecast Skill

2.2.1 Methods Employed in Previous Work

To interpret the utility of any tentative forecast method, a quantitative means of assessing the skill of that method must be implemented. The methods of skill assessment developed in previous work are here reviewed.

Four complementary skill indicators have come to be used in assessing useful multiple regression predictor combinations. First, apparently skilful individual predictors are identified on the basis of relatively large correlation coefficients emerging from linear regression tests between predictor eigenfunction coefficients and ice indices. Predictor time domains employed in past east coast iceberg and sea ice work have ranged from 22 to 39 years depending on the availability of predictor data fields and the duration of the predictand data record. Potentially useful predictors thus identified are tested by performing a 22 to 39 year dependent hindcast, and comparing the results of this hindcast against actual ice index occurrence values.

A second coarse measure of predictive skill in such a hindcast is obtained by dividing the forecast domain into terciles (one third least severe, one third moderate, and one third most severe years). The available years of predictions are ranked by increasing ice index value and are separated into three equally sized sets. For example, with 30 years of predictor data, the three sets would be defined as ranks 1 to 10, 11 to 20, and 21 to 30. Tercile errors are then computed. Again, using the 30 year example, years with observed rank 1 to 10 and predicted rank 1 to 10 would yield an error of 0. These are termed "Category Errors". Pursuing this same example, a prediction of 21 to 30 for an observed rank of 1 to 10 would yield a Category Error of 2. Experience in the use of these Category Error skill indicators has shown that unless

there is uniform year to year variation in the ice severity index (which condition is virtually never met), this method is rather poor for discriminating true forecast accuracy in the first and second terciles. The true merit of a tercile Category Error scheme has been shown to lie in the number of predicted cases with Category Error = 2. Actual forecasts (hindcasts) which yield low (or ideally zero) values of Category Error = 2 can be regarded as demonstrating true skill.

Thirdly, more refined classification schemes than the tercile ranking have been introduced. With such schemes it is possible to illustrate the skill of a prediction using absolute Class Error as an indicator. This is simply the numerical absolute value of the difference between predicted and observed class. One of two classification schemes for sea ice area indices is commonly employed, depending on the mean ($\bar{x}$) and standard deviation (σ) values of the area index. These computed class definitions are specified in Table 2.1.

Table 2.1 Definition of Sea Ice Severity Classes

Class	1	2	3	4	5
Upper Bound	$-\infty$	$\bar{x}-\sigma$	$\bar{x}-\frac{1}{2}\sigma$	$\bar{x}+\frac{1}{2}\sigma$	$\bar{x}+1\frac{1}{2}\sigma$
Lower Bound	$\bar{x}-\sigma$	$\bar{x}-\frac{1}{2}\sigma$	$\bar{x}+\frac{1}{2}\sigma$	$\bar{x}+1\frac{1}{2}\sigma$	∞

or, for $\sigma/\bar{x} \geq 2$ =

Class	1	2	3	4	5
Upper Bound	$-\infty$	$\bar{x}-\sigma$	$\bar{x}-\frac{1}{2}\sigma$	$\bar{x}$	$\bar{x}+1\frac{1}{2}\sigma$
Lower Bound	$\bar{x}-\sigma$	$\bar{x}-\frac{1}{2}\sigma$	$\bar{x}$	$\bar{x}+1\frac{1}{2}\sigma$	∞

The same principle described above for tercile category error distributions is applicable with class error distributions: true forecast skill is manifested by the minimal occurrence of class errors in the higher (class error $\geq$ 3) divisions.

Fourthly, and finally, a rank error index (called Delta Rank) is in use. This latter factor is assessed by computing the difference between observed and hindcast severity rank (least severe year has rank 1 and most severe year in an n year population has rank n). Small values of this Delta Rank parameter indicate that severe years are being hindcast correctly.

These four skill indicators appear on every printed sheet of hindcast results output from LRIFS. Table 2.2 is provided to illustrate the format in which hindcast results are printed, and to identify the location of the four skill indicators on a typical output sheet. This sample is included to illustrate format: the numerical content of the sample provided in Table 2.2 is arbitrary, and of no technical importance.

Table 2.2 Sample Multiple Regression Output With Four Skill Indicators Highlighted

DEPENDENT COMPARISON OF OBSERVED SEA ICE AREA VS PREDICTED SEA ICE AREA
FOR SOUTH REGION BOUNDED BY 44 - 56 W AND 43 - 52 N
FOR ICE CONDITIONS SPANNING 1 MONTH(S) ENDING IN JANUARY

Region : new_data
Latitude : 45 to 90 Deg. N
Issue Date : January 1st
MLR Equation # 1

Size : 10 x 10
Longitude : 10 to 100 Deg. W
Run Date : 13:55:41 25-Jan-93

Predictor	# Months	Ending In
Mean Sea Level Pressure	1	December A(1)
Surface Air Temperature	6	December A(1)
Surface Air Temperature	2	December A(2)

1

Correlation Coefficient : .65

YEAR	OBSERVED	PREDICTED	(P-O)	OBS RANK	PRED RANK	DELTA RANK
1969	5427.	27504.	22078.	1.	11.	10.
1982	5572.	0.	-5572.	2.	1.	-1.
1966	6721.	13159.	6438.	3.	5.	2.
1978	8114.	28574.	20461.	4.	12.	8.
1963	9082.	13336.	4254.	5.	6.	1.
1970	11153.	4171.	-6982.	6.	3.	-3.
1979	13126.	22917.	9791.	7.	9.	2.
1964	13870.	16406.	2536.	8.	8.	0.
1968	14201.	15272.	1071.	9.	7.	-2.
1962	15748.	0.	-15748.	10.	2.	-8.
1980	16450.	39076.	22626.	11.	19.	8.
1981	16457.	38098.	21641.	12.	18.	6.
1967	17057.	24893.	7836.	13.	10.	-3.
1975	18410.	30267.	11857.	14.	14.	0.
1965	18572.	31800.	13227.	15.	15.	0.
1976	20893.	36830.	15937.	16.	17.	1.
1971	22213.	30079.	7866.	17.	13.	-4.
1977	23084.	34324.	11239.	18.	16.	-2.
1972	43093.	47907.	4814.	19.	20.	1.
1974	44034.	8684.	-35350.	20.	4.	-16.
1983	45903.	50653.	4749.	21.	21.	0.
1973	164197.	68023.	-96174.	22.	22.	0.
MEAN	25153.	26453.				
STD. DEV.	33178.	17046.				
MEAN OF ABSOLUTE VALUES			11084.			2.8
STD. DEV. OF ABSOLUTE VALUES			7184.			3.6

4

CATEGORY ERRORS: DISCREPANCY BETWEEN OBSERVED AND PREDICTED CATEGORIES

	COUNT
0	13
1	8
2	1

2

CLASS ERRORS: DISCREPANCY BETWEEN OBSERVED AND PREDICTED CLASSIFICATION

	COUNT	CHANCE ERROR
0	15	5.5
1	7	9.8
2	0	5.5
3	0	1.3

3

2.2.2 Composite Skill Index

The four indicators described above have been employed in previous studies to search for potentially viable individual predictors. Once isolated, these apparently skilful predictors have then been judiciously grouped to test various multiple regression combinations. This two-step process has required considerable manual/visual assessment, ultimately demanding subjective judgement on the basis of these four skill indicators, to isolate most desirable sets of predictors. In the first step, decisions were required to define groupings of the predictors which evolve from the linear regression tests. In the second step, the output from each multiple regression test was visually assessed against hindcast results from other multiple regression combinations (for a given region, predictand, and time interval) to select the apparently best combinations. In a most significant change to the LRIFS system, an objective Composite Skill Index has been developed, tested, and implemented so as to streamline the human intervention and decision making required in isolating useful forecast equations. Implementation of the Composite Skill Index (CSI) allows all possible combinations of predictors to be investigated, with only the apparently most skilful predictor combinations then saved for final human inspection and acceptance.

The composite skill index incorporates the four skill indicators in the manner described in Table 2.3. The composite skill index does not in any sense eliminate the need for human assessment of hindcast results as skilful equations are being sought, but it provides a single quantitative parameter by which to rank the results of hindcast tests using thousands of potential equations. In this manner, it focuses human attention on the few best possible equations.

Current practice is to employ the CSI to isolate up to ten individual predictors for each meteorological parameter for each combination of region, predictand, and issue date. With certain defined constraints about allowable combinations, all possible multiple regression combinations of these isolated individual predictors are then assessed. For each region, predictand, and issue date, up to the 50 best combinations are saved, ranked by CSI. The sole human judgement required in the present configuration, then, is to review these 50 (or less) equations, and to identify those three which are to be retained in the operational forecast equation matrix.

2.3 Northern Hemisphere Expansion of Predictor Domain

Just as the ability to automatically identify and rank high quality forecast equations has evolved over the years that this work has been active, so has the flexibility to select geographical boundaries for the predictor region improved. In the earliest iceberg work, an arbitrarily defined region spanning 50° latitude by 100° longitude, centred over the Labrador Sea, was the sole option. As the system was expanded to incorporate the ability to forecast east coast sea ice severity, geographical flexibility was also added. It was then possible to define any square predictor grid within a 15 x 15 element domain defined by latitudes 20° N and 90° N, and by longitudes 0° W and 140° W. Allowable predictor grids were tested with sizes 6 x 6 through 15 x 15, at various locations within this maximum 15 x 15 domain.

Table 2.3 **Definition of Composite Skill Index (CSI)**

Indicator	CSI Contribution	Comments on method of inclusion in CSI
Correlation Coefficient	30%	absolute value of "r" contributes to CSI.
Category error	20%	contribution drops off as the square of the number of events with category error of 2, and is adjusted marginally for differences between number of events with category error of zero or 1.
Class error	20%	contribution drops off as the square of the number of events with class error of 4 or greater, and is adjusted with proportionally lighter weights for differences between number of events with class error of zero through 3.
Delta rank	30%	contribution decays in approximate linear fashion based on number of the five events which have rank errors, and on the magnitude of those errors.

The weightings for the four components of the CSI are adjustable. All results included in this report employ the [30%, 20%, 20%, 30%] scheme noted above.

A major accomplishment of the present work has been to expand the available predictor domain to span the entire Northern Hemisphere. All predictor data sets have been updated for the entire hemisphere (see Chapter 4.2), and a practical menu interface has been added to LRIFS to allow maximum flexibility in user definition of the geographical region for calculation of predictor eigenfunctions.

2.4 Confirmation of System Compatibility

Significant activities completed in connection with the present work have included introduction of the Composite Skill Index (Chapter 2.2.2) with partial automation of equation selection, expansion of the predictor domain to span the entire Northern Hemisphere (Chapter 2.3), updating and partial replacement of most meteorological predictor files (Chapter 4.2), and major modifications to the LRIFS User Interface (Pinhorn, 1993b). The LRIFS package has also been moved to a new host computer system. Most of these activities represent major structural changes to LRIFS. To verify the proper functioning of LRIFS after all of these changes had been made was deemed to be a critical requirement. Three examples of such verification work are here provided to document the compatibility between the present version of LRIFS, and versions which had previously been considered to be ready (or near-ready) for operational forecast use.

2.4.1 Linear Regression Compatibility Test for Iceberg Flux Hindcast

Linear regression tests for MSLP 4 months ending March a(1) to hindcast iceberg flux are shown in Table 2.4. The left panel of this table is a direct reproduction of Table I.3(a) from Page 137 of Davidson et al. (1986). The right panel is output from LRIFS generated January 26, 1993. Virtually the same MSLP data sets contribute to each of these hindcasts, as no changes to the LRIFS MSLP data holdings have been made since 1984. Values of predicted iceberg flux in each of the two cases are nearly identical. A corrected value of actual flux for 1962 (changed for 112 to 122) causes minor differences in the Predicted Rank and Delta Rank statistics, and these are sufficient to cause minor changes in the counts for Class Error = 2. The counts for Category Error and the Correlation Coefficient are exactly the same in both panels. This table provides tangible evidence of compatibility in MSLP linear regressions in spite of the enormous system changes which have been implemented between 1986 and 1993.

2.4.2 Multiple Regression Compatibility Test for Iceberg Flux Hindcast

Results of a five parameter combination used to predict iceberg flux are shown in Table 2.5. The left panel of this table is a direct reproduction of Table I.10(b) from Page 153 of Davidson et al. (1986). The right panel is output from LRIFS generated January 26, 1993. The 700 mb height data and the 700 - 1000 mb thickness data contributing to this multiple regression test have undergone minor changes since 1986. Copies of these time series data from multiple sources have been recombined in different groupings of years than was the case in 1986. Again, however, the columns of predicted iceberg flux values in these two panels show excellent correspondence in magnitude and especially in trend. Again the correlation coefficient is unchanged. Even though there are clearly noticeable difference in the Category Error and Class Error tables, these differences have little effect on the actual assessment which would be made

Table 2.4 Linear Regression Compatibility Test for Iceberg Hindcast
Left Panel From Davidson et al. (1986) and Right Panel From Current Work

DEPENDENT COMPARISON OF OBSERVED ICEBERG FLUX VS PREDICTED ICEBERG FLUX

Parameter : MEAN SEA LEVEL PRESSURE TIME AVERAGED APPROACH

Number of Months: 4 Correlation Coefficient r: -.49
Ending in : MARCH

YEAR	a(1)	OBSERVED	PREDICTED	(P-O)	(P-O / SD)	OBS RANK	PRED RANK	DELTA RANK
1966	42.28	0.	11.	11.	.03	1.	3.	2.
1958	35.16	1.	57.	56.	.14	2.	6.	4.
1952	22.02	15.	142.	127.	.31	3.	9.	6.
1977	39.25	22.	30.	8.	.02	4.	4.	0.
1980	-17.09	23.	396.	373.	.91	5.	20.	15.
1963	4.38	25.	257.	232.	.56	6.	14.	8.
1953	-15.37	56.	385.	329.	.80	7.	19.	12.
1969	50.80	57.	0.	-57.	-.14	8.	1.	-7.
1955	23.06	61.	136.	75.	.18	9.	8.	-1.
1971	12.70	73.	203.	130.	.31	10.	11.	1.
1978	6.71	75.	242.	167.	.40	11.	13.	2.
1965	1.76	76.	274.	198.	.48	12.	15.	3.
1956	-3.79	80.	310.	230.	.56	13.	16.	3.
1970	20.62	85.	151.	66.	.16	14.	10.	-4.
1975	-21.05	101.	422.	321.	.78	15.	22.	7.
1962	36.13	112.	51.	-61.	-.15	16.	5.	-11.
1961	-14.03	114.	377.	263.	.64	17.	18.	1.
1976	-64.98	151.	708.	557.	1.35	18.	29.	11.
1979	30.22	182.	89.	-93.	-.23	19.	7.	-12.
1968	8.51	226.	230.	4.	.01	20.	12.	-8.
1960	42.35	258.	10.	-248.	-.60	21.	2.	-19.
1954	-49.06	312.	604.	292.	.71	22.	28.	6.
1964	-34.07	369.	507.	138.	.33	23.	26.	3.
1967	-28.82	441.	473.	32.	.08	24.	23.	-1.
1959	-17.81	689.	401.	-288.	-.70	25.	21.	-4.
1973	-47.72	850.	596.	-254.	-.62	26.	27.	1.
1957	-10.59	931.	354.	-577.	-1.40	27.	17.	-10.
1974	-30.35	1386.	483.	-903.	-2.19	28.	24.	-4.
1972	-33.23	1584.	501.	-1083.	-2.62	29.	25.	-4.
MEAN		288.	288.					
STD. DEV.		413.	203.					
MEAN OF ABSOLUTE VALUES				247.4	.60			5.9
STD. DEV. OF ABSOLUTE VALUES				255.4	.62			4.8

CATEGORY ERRORS: DISCREPANCY BETWEEN OBSERVED AND PREDICTED CATEGORIES	COUNT
0	18
1	10
2	1

CLASS ERRORS: DISCREPANCY BETWEEN OBSERVED AND PREDICTED CLASSIFICATION	COUNT
0	5
1	10
2	11
3	3
4	0
5	0
6	0

DEPENDENT COMPARISON OF OBSERVED ICEBERG FLUX VS PREDICTED ICEBERG FLUX

Latitude : 45 to 90 Deg. N Longitude : 10 to 100 Deg. W
Region : data_test Run Date : 10:25:39 26-Jan-93

Predictor : MEAN SEA LEVEL PRESSURE
Number of Months: 4 Correlation Coefficient r: -.49
Ending in Month : MARCH Composite Skill Index : .42

YEAR	a(1)	OBSERVED	PREDICTED	(P-O)	OBS RANK	PRED RANK	DELTA RANK
1966	42.23	0.	9.	9.	1.	3.	2.
1958	35.12	1.	56.	55.	2.	6.	4.
1952	21.98	15.	141.	126.	3.	9.	6.
1977	39.21	22.	29.	7.	4.	4.	0.
1980	-17.13	23.	396.	373.	5.	20.	15.
1963	4.33	25.	256.	231.	6.	14.	8.
1953	-15.42	56.	385.	329.	7.	19.	12.
1969	50.76	57.	0.	-57.	8.	1.	-7.
1955	23.02	61.	134.	73.	9.	8.	-1.
1971	12.65	73.	202.	129.	10.	11.	1.
1978	6.66	75.	241.	166.	11.	13.	2.
1965	1.71	76.	273.	197.	12.	15.	3.
1956	-3.83	80.	309.	229.	13.	16.	3.
1970	20.58	85.	150.	65.	14.	10.	-4.
1975	-21.10	101.	422.	321.	15.	22.	7.
1961	-14.08	114.	376.	262.	16.	18.	2.
1962	36.09	122.	49.	-73.	17.	5.	-12.
1976	-65.02	151.	708.	557.	18.	29.	11.
1979	30.18	152.	88.	-64.	19.	7.	-12.
1968	8.47	226.	229.	3.	20.	12.	-8.
1960	42.30	258.	9.	-249.	21.	2.	-19.
1954	-49.10	312.	605.	293.	22.	28.	6.
1964	-34.12	369.	507.	138.	23.	26.	3.
1967	-28.86	441.	473.	32.	24.	23.	-1.
1959	-17.85	689.	401.	-288.	25.	21.	-4.
1973	-47.76	850.	596.	-254.	26.	27.	1.
1957	-10.63	931.	354.	-577.	27.	17.	-10.
1974	-30.39	1386.	483.	-903.	28.	24.	-4.
1972	-33.27	1584.	501.	-1083.	29.	25.	-4.
MEAN		287.	289.				
STD. DEV.		413.	201.				
MEAN OF ABSOLUTE VALUES				180.			5.1
STD. DEV. OF ABSOLUTE VALUES				146.			4.3

CATEGORY ERRORS: DISCREPANCY BETWEEN OBSERVED AND PREDICTED CATEGORIES	COUNT
0	18
1	10
2	1

CLASS ERRORS: DISCREPANCY BETWEEN OBSERVED AND PREDICTED CLASSIFICATION	COUNT
0	5
1	14
2	7
3	3
4	0
5	0

Table 2.5 Multiple Regression Compatibility Test for Iceberg Hindcast
Left Panel From Davidson et al. (1986) and Right Panel From Current Work

DEPENDENT COMPARISON OF OBSERVED ICEBERG FLUX VS PREDICTED ICEBERG FLUX

TIME AVERAGED APPROACH

PARAMETER	NUMBER OF MONTHS	ENDING IN	a(n)	r
700 MB HEIGHTS	5	DECEMBER	5	-.58
700 MB HEIGHTS	2	OCTOBER	3	-.57
700 - 1000 MB THICKNESS	2	DECEMBER	4	-.54
MEAN SEA LEVEL PRESSURE	4	DECEMBER	5	.55
MEAN SEA LEVEL PRESSURE	2	JANUARY	1	-.49

Correlation Coefficient (Observed vs Predicted): .81

YEAR	OBSERVED	PREDICTED	(P-O)	(P-O / SD)	OBS RANK	PRED RANK	DELTA RANK
1966	0.	84.	84.	.20	1.	10.	9.
1958	1.	165.	164.	.40	2.	11.	9.
1952	15.	337.	322.	.78	3.	19.	16.
1977	22.	0.	-22.	-.05	4.	3.	-1.
1980	23.	18.	-5.	-.01	5.	6.	1.
1963	25.	255.	230.	.56	6.	17.	11.
1953	56.	224.	168.	.41	7.	15.	8.
1969	57.	0.	-57.	-.14	8.	1.	-7.
1955	61.	0.	-61.	-.15	9.	4.	-5.
1971	73.	169.	96.	.23	10.	13.	3.
1978	75.	0.	-75.	-.18	11.	5.	-6.
1965	76.	566.	490.	1.19	12.	24.	12.
1956	80.	306.	226.	.55	13.	18.	5.
1970	85.	70.	-15.	-.04	14.	8.	-6.
1975	101.	239.	138.	.33	15.	16.	1.
1962	112.	0.	-112.	-.27	16.	2.	-14.
1961	114.	168.	54.	.13	17.	12.	-5.
1976	151.	551.	400.	.97	18.	23.	5.
1979	182.	338.	156.	.38	19.	20.	1.
1968	226.	71.	-155.	-.38	20.	9.	-11.
1960	258.	28.	-230.	-.56	21.	7.	-14.
1954	312.	573.	261.	.63	22.	25.	3.
1964	369.	372.	3.	.01	23.	21.	-2.
1967	441.	213.	-228.	-.55	24.	14.	-10.
1959	689.	543.	-146.	-.35	25.	22.	-3.
1973	850.	718.	-132.	-.32	26.	26.	0.
1957	931.	805.	-126.	-.30	27.	27.	0.
1974	1386.	1135.	-251.	-.61	28.	29.	1.
1972	1584.	992.	-592.	-1.43	29.	28.	-1.
MEAN	288.	288.					
STD. DEV.	413.	336.					
MEAN OF ABSOLUTE VALUES			172.	.42			5.9
STD. DEV. OF ABSOLUTE VALUES			141.	.34			4.7

CATEGORY ERRORS: DISCREPANCY BETWEEN OBSERVED AND PREDICTED CATEGORIES	COUNT
0	16
1	12
2	1

CLASS ERRORS: DISCREPANCY BETWEEN OBSERVED AND PREDICTED CLASSIFICATION	COUNT
0	7
1	12
2	6
3	4
4	0
5	0
6	0

DEPENDENT COMPARISON OF OBSERVED ICEBERG FLUX VS PREDICTED ICEBERG FLUX

Region : data_test
Latitude : 45 to 90 Deg. N
Issue Date : January 1st
MLR Equation # 2

Size : 10 x 10
Longitude : 10 to 100 Deg. W
Run Date : 12:28:35 26-Jan-93

Predictor	# Months	Ending In
H700 (Walsh & NCAR Joined)	5	December A(5)
H700 (Walsh & NCAR Joined)	2	October A(3)
D700 (From J1000 & J700)	2	December A(4)
Mean Sea Level Pressure	4	December A(5)
Mean Sea Level Pressure	2	January A(1)

Correlation Coefficient : .81 Composite Skill Index : .66

YEAR	OBSERVED	PREDICTED	(P-O)	OBS RANK	PRED RANK	DELTA RANK
1966	0.	85.	85.	1.	9.	8.
1958	1.	187.	186.	2.	13.	11.
1952	15.	318.	303.	3.	18.	15.
1977	22.	0.	-22.	4.	3.	-1.
1980	23.	32.	9.	5.	7.	2.
1963	25.	217.	192.	6.	15.	9.
1953	56.	213.	157.	7.	14.	7.
1969	57.	0.	-57.	8.	2.	-6.
1955	61.	0.	-61.	9.	5.	-4.
1971	73.	155.	82.	10.	12.	2.
1978	75.	95.	20.	11.	10.	-1.
1965	76.	592.	516.	12.	25.	13.
1956	80.	339.	259.	13.	19.	6.
1970	85.	13.	-72.	14.	6.	-8.
1975	101.	243.	142.	15.	16.	1.
1961	114.	291.	177.	16.	17.	1.
1962	122.	0.	-122.	17.	4.	-13.
1976	151.	471.	320.	18.	22.	4.
1979	152.	373.	221.	19.	21.	2.
1968	226.	0.	-226.	20.	1.	-19.
1960	258.	75.	-183.	21.	8.	-13.
1954	312.	524.	212.	22.	24.	2.
1964	369.	362.	-7.	23.	20.	-3.
1967	441.	142.	-299.	24.	11.	-13.
1959	689.	489.	-200.	25.	23.	-2.
1973	850.	916.	66.	26.	28.	2.
1957	931.	831.	-100.	27.	26.	-1.
1974	1386.	1000.	-386.	28.	29.	1.
1972	1584.	877.	-707.	29.	27.	-2.
MEAN	287.	305.				
STD. DEV.	413.	300.				
MEAN OF ABSOLUTE VALUES			184.			5.4
STD. DEV. OF ABSOLUTE VALUES			128.			4.6

CATEGORY ERRORS: DISCREPANCY BETWEEN OBSERVED AND PREDICTED CATEGORIES	COUNT
0	14
1	14
2	1

CLASS ERRORS: DISCREPANCY BETWEEN OBSERVED AND PREDICTED CLASSIFICATION	COUNT
0	7
1	14
2	6
3	2

of the utility of this forecast equation. Both incarnations of this test return one year with Class Error = 1. The more recent case returns only two years with Category Error = 3, while the former version returned four years in this error category. The rank differences for the five most severe years fluctuate by no more than two units. These illustrated results, in company with the results of many comparable tests not illustrated here, confirm the compatibility between the 1986 version of LRIFS and the version which has emerged following the major upgrading activities described in this report.

2.4.3 Compatibility Tests Using East Coast Sea Ice Hindcasts

Further confirmation of the compatibility between the current version of LRIFS and the operational version reported to Ice Centre Environment Canada by Davidson (1992) is provided in Table 2.6. In this instance, four different multiple regression combinations are tested for the prediction of Grand Banks sea ice severity. Correlation coefficients, Category Error distributions, Class Error distributions, and Delta Rank statistics are compared for each of the four multiple regression cases, each for a different issue date. Over the past year, the contributing data files for H1000, H500, and D500 have undergone considerable revisions in term of source and time groupings of data (see Chapter 4.2). In spite of these changes to the basic predictor data files, LRIFS returns acceptably compatible results in each of the four tests. The pairs of Correlation Coefficients match to within 0.02 in Tests #1, #2 and #4, while Test #3 presents a difference of only 0.09. Conspicuous in Test #1 is the large Delta Rank error in the third most severe year. This shows as an error of -18 in 1992 and is reproduced as a comparable error of -16 in 1993. In Test #2 the Category Error and Class Error distributions are identical for the two cases. In this instance there is somewhat larger fluctuation in Delta Rank. In spite of the Correlation Coefficient differences in Test #3 there is excellent compatibility in all three other skill indicators. Finally, in Test #4, there is again a recognizable pattern in the behaviour of each of the skill indicators for the two cases (1992 and 1993 versions of LRIFS).

2.5 Isolating Useful Predictors

2.5.1 Problems with Artificial Skill

Attempts to develop skilful forecast equations from meteorological predictors, for any particular ice predictand, always follow a basic series of steps. A geographical region is first selected, in which to base the search for skilful meteorological predictors. Linear regression tests between eigenfunction coefficient time series and predictand time series are used to isolate individually interesting predictors. These are then combined in various groupings to test multiple regression models. Chapter 2.2.2 above has introduced the Composite Skill Index (CSI) as a quantitative tool for assessing the skill of both linear and multiple regression tests. With the introduction of the CSI, and with advances in computing throughput, it has become practical to test virtually every possible linear regression option, and likewise to test every possible multiple regression combination if desired.

In a typical case, with no unusual restrictions, the number of possible linear regression tests for a given geographical predictor domain, a given ice predictand, and a given issue date, could be

Table 2.6 Comparison of Four Multiple Regression Predictor Combinations Using LRIFS 1992 and 1993 Versions

Equation	Predictand				Predictors				Results											
Number	R	Index	#mos	End	P	#mos	End	a(n)	r	Category			Class					Delta Rank				
Test #1a 1992	S	ICEA	1	Jan	MSLP	1	Dec	1	0.67	12	8	2	14	7	1	0		0	0	-18	-1	-4
					SAT	6	Dec	1														
					Sat	2	Dec	2														
Test #1b 1993									0.65	13	8	1	15	7	0	0		-2	1	-16	0	0
Test #2a 1992	S	ICEA	1	Feb	D500	3	Jan	1	0.89	15	6	1	14	8	0	0	0	-2	1	1	-1	-5
					H500	2	Jan	2														
					H1000	2	Jan	1														
					H1000	5	Jan	3														
					SAT	2	Jan	1														
Test #2b 1993									0.89	15	6	1	14	8	0	0	0	-6	0	1	1	-2
Test #3a 1992	S	ICEA	1	Mar	D500	3	Feb	1	0.91	14	8	0	17	5	0	0	0	0	0	-2	-2	1
					D500	3	Feb	2														
					H500	3	Feb	1														
					H1000	2	Feb	1														
					SAT	3	Feb	1														
Test #3b 1993									0.85	13	8	1	15	7	0	0	0	1	-2	-2	0	0
Test #4a 1992	S	ICEA	1	Apr	D500	4	Mar	1	0.76	14	8	0	13	8	1	0	0	-1	-4	0	3	-3
					D500	4	Mar	2														
					H700	4	Mar	1														
					MSLP	4	Mar	1														
					SAT	4	Mar	1														
Test #4b 1993									0.76	12	10	0	9	12	1	0	0	-3	1	2	-4	-1

as large as:

	7	meteorological predictors
x	6	eigenfunction modes saved for each predictor
x	8	number of months contributing to predictor average
x	12	(or less) end month *
	4,032	maximum number of linear regression cases

* Not all cases are allowed to extend back a full twelve months in time. For the Beaufort Sea, for example, November has been determined as the transition month between ice seasons, so linear regression tests for say a July 1 issue date would extend back only eight months to the previous November, and not 12 months to the previous July.

In any event, some few thousands of linear regression tests are executed for each region/predictand/issue date combination. It has become common practice to retain up to ten cases for each of the seven meteorological fields which yield the maximum CSI values, provided that at least ten cases pass the equal-tails test for significance of the correlation coefficient (Neville and Kennedy, 1966).

As this method evolved and was being assessed, it became apparent from many test results that certain predictors were being retained which did not spontaneously have a reasonable physical explanation. Illustrative of many such results encountered in the early phases of this work is the example cited in Table 2.7. Viewed in conjunction with similar lists for earlier issue dates, it is difficult to offer a plausible physical explanation for the apparent skill in predictors which have both a long lead time and a high mode number. Thus, the two April a(4) predictors and especially the January a(3) predictor in Table 2.7 were viewed with scepticism, even though being retained by the automatic selection system.

With almost all linear regression tests plagued by some number of these questionable predictors showing what could be artificial skill, it was determined to add another rigorous skill test to the linear regression module of LRIFS. This Monte Carlo simulation test (described immediately below in Chapter 2.5.2) is so computationally intensive that it cannot be invoked with every linear regression test. Therefore, arbitrary but reasonable rules to control the execution of Monte Carlo tests have been established as follows:

- a predictor from the list of ten largest CSI values is spontaneously retained on the list if its end month is only one or two months earlier than the issue date.

- any predictor having an end month which is three or more months prior to the issue date must be subjected to the Monte Carlo test.

Table 2.7 **Example of Linear Regression Results Including Questionable Predictors**

In this example:

Region	=	Beaufort Sea 10 X 10 E 40°N to 90°N latitude 90°W to 180°W longitude
Predictand	=	Beaufort Sea Ice Area 1 month ending July
Issue Date	=	July 1

Linear Regression Results for 700 mb Height as follows:

Potential Predictor	CSI	r	Duration	End month	Coefficient Series
1	.71	.68	2	June	a(1)
2	.70	-.62	3	June	a(1)
* 3	.68	.64	1	April	a(4)
* 4	.68	.61	2	April	a(4)
* 5	.64	.55	4	January	a(3)
6	.62	-.58	1	June	a(1)
7	.60	.60	4	June	a(1)
8	.56	.58	5	June	a(1)
9	.51	-.59	4	June	a(6)

* It is difficult to physically explain these predictors with both long lead time and high mode number.

- a predictor from the list of ten largest CSI value is spontaneously retained on the list i it employs eigenfunction mode 1 or mode 2.

- any predictor employing eigenfunction mode 3 or higher must be subjected to the Mont Carlo test, independent of its end month.

2.5.2 Monte Carlo Techniques

To further assess predictors showing potentially artificial skill (as defined above), a rigorous Monte Carlo test was added to the linear regression module of LRIFS. The implementation of this test is described as follows:

- first, the standard approach to predictor selection for the given predictor and month is undertaken, by regressing the ice area signal against each of the 48 a(n) series. Thus, apparent predictors are identified. If any of these are for modes of the eigenfunction which are greater than 2, or if any of the predictors have end dates which are more than two months earlier than the issue date, then the Monte Carlo test is executed.

- for a given meteorological predictor field (MSLP, H1000, H700, etc.) and a given month, there are 48 combinations of duration and eigenfunction coefficient which are normally investigated to seek viable predictors. These 48 cases are illustrated in Table 2.8 below.

Table 2.8 Allowable Combinations of Duration and Eigenfunction Coefficient

Eigenfunction Coefficient a(n)	Number of Months Duration 1	2	3	4	5	6	7	8
a(1)								
a(2)	This matrix defines 48 combinations of duration and							
a(3)	eigenfunction coefficient.							
a(4)								
a(5)								
a(6)								

- a "chance" distribution of CSI values is constructed. First, the ice area index series is randomized. This random ice signal is regressed against all 48 of the above-defined potential predictor series. The single largest of the 48 CSI values resulting from this computation is retained. The process is repeated 100 times, each with a different randomized version of the ice area series. This yields a population of 100 CSI values, all derived from randomized ice signals.

- the 95% threshold in that distribution of 100 CSI values is determined.

- for the questionable predictor to be retained, its CSI value must exceed the 95% threshold value from the distribution of 100 CSI values generated by random ice signals.

Examples of the consequence of imposing the Monte Carlo test are illustrated in Figure 2.1. The Figure comprises four cases, each of which involves an apparently skilful, but suspect predictor, with the suspicions arising from the mode of eigenfunction being greater than 2, or the end date being more than two months earlier than the issue date. In this early example, the threshold for retention of suspicious predictors was set at 90% in the distribution of random CSI values. This threshold applies to the results in Figure 2.1. Subsequently, as noted above, the threshold was raised to 95% to tighten the condition for retention of predictors. It is noted that in this example, three of the four illustrated examples fail the Monte Carlo test, while one (June) passes.

Figure 2.1 Examples of Monte Carlo Tests for Predictor Viability

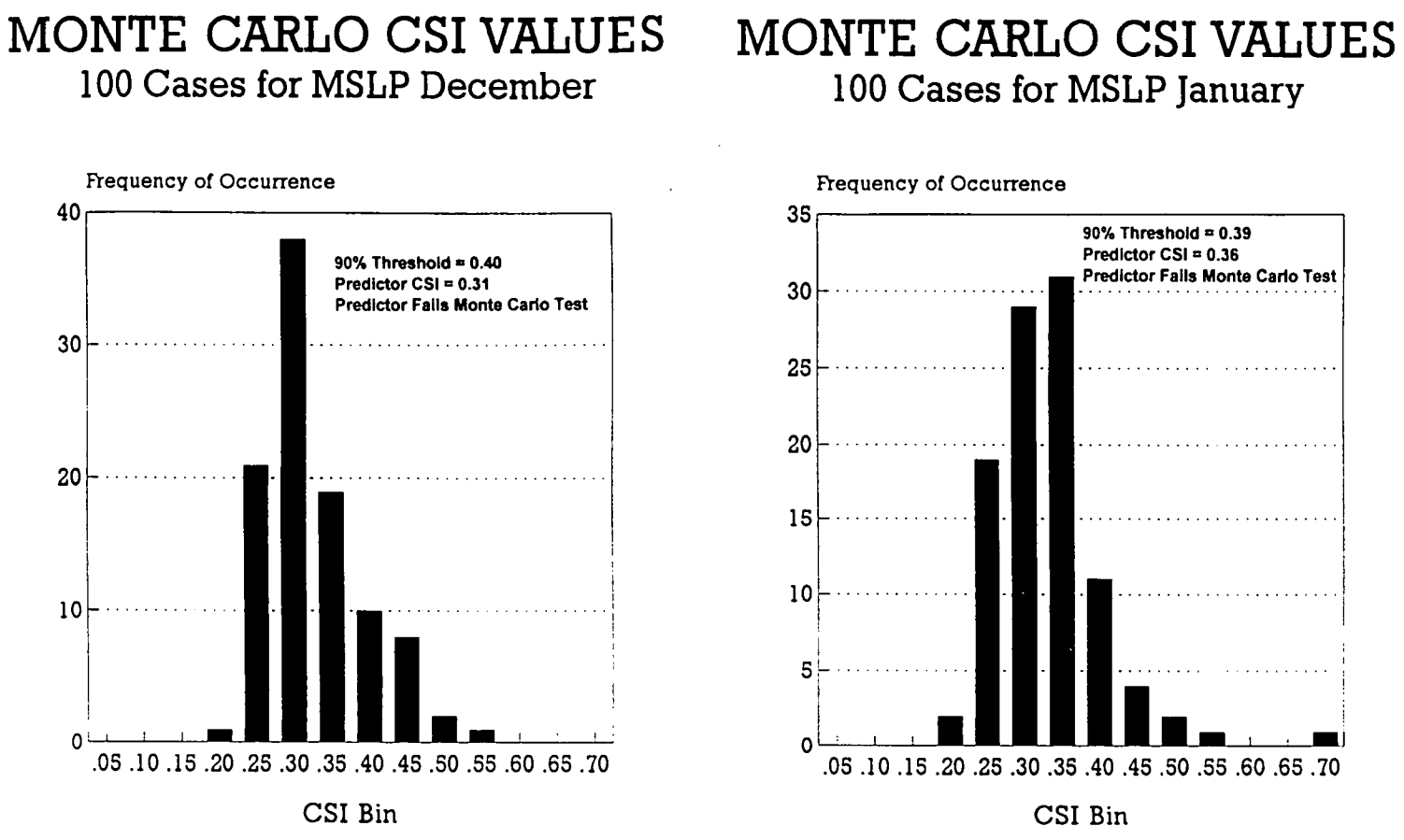

2.6 Summary of Modified LRIFS System Operation

It is the purpose of the associated User's Manual for LRIFS (Pinhorn, 1993b), to provide comprehensive documentation for the guidance of system users. Repetition of such information in this technical report is inappropriate. However, it is appropriate here to provide a summary of the process by which predictive equations are derived, using the LRIFS system. Such a summary if provided via Table 2.9.

Table 2.9 Summary of the Process for Equation Generation in the Modified Long Range Ice Forecasting System

Action Taken By	Input Parameter or Computational Action	Range of Values Presently Supported
User	Define the geographical region for the meteorological predictor grid. Once this highest level menu selection establishes a predictor region, the system allocates initial space required for development and storage of forecast equations, and all subsequent user choices pertain to this region. The LRIFS system now supports multiple regions simultaneously, constrained only by total system disk space.	Allowable predictor regions are any square grid (composed of 5° latitude by 10° longitude cells), dimensioned 6 X 6 through 15 X 15, and located anywhere north of 20° N latitude in the northern hemisphere.
User	Choose meteorological predictors and the range of years for inclusion in the computation of eigenfunctions for each predictor.	Seven options are available, including: - mean sea level pressure (MSLP) - 1000 millibar geopotential height(H1000) - 700 millibar geopotential height (H700) - 500 millibar geopotential height (H500) - 700-1000 millibar thickness (D700) - 500-1000 millibar thickness (D500) - surface air temperature (SAT) Any continuous range of years, within the available time range of data for each parameter, is allowable. Different ranges of years can be set independently for each selected meteorological field, if desired.
User	Select antecedent ice index as a predictor if desired.	Any of the currently defined ice index series can optionally be included in the predictor list.
Automatic	Compute and store monthly means for each selected meteorological predictor time series.	
User	Set the time grouping parameters for eigenfunction generation.	Options are 1 to 8 months ending January to December (maximum 8 X 12 = 96 cases), or any subset thereof.
Automatic	Compute eigenfunctions for each selected predictor and time grouping. Store the first six eigenfunctions with their eigenvalues. Compute and store the eigenfunction coefficient time series (a_n), which is the information used in linear regression tests against the ice index series.	
User	Select predictors for inclusion in linear regression tests.	Options are any combination of the meteorological and ice predictors identified above. In a typical use of the system, the first action for a newly defined region would be to select all predictors and execute all eigenfunction computations. Subsequently, this selection option would be used to investigate specific sets of predictors.

Table 2.9 (cont.)

User	Choose predictand series.	Options are any currently defined ice index series.
User	Choose ice signal (predictand) duration and end month.	Duration options for sea ice are one month or three months, while for icebergs the duration is always annual. Options for end month for the sea ice signal are region specific. Allowable values currently include: East Coast: North August through July Middle August through July South December through July Gulf December through July Beaufort Sea: June through October
Automatic	Execute every possible linear regression test between ice predictand series and predictor series, as dictated by the population of stored eigenfunctions, and the selected predictor series. Execute Monte Carlo tests to filter questionable apparent predictors. Construct and store lists of the 10 best linear predictors as determined by values of the Composite Skill Index (CSI).	Monte Carlo tests are executed if lead time is greater than 2 months or if eigenfunction mode is 3 or greater.
User	Define an issue date. This controls which lists of 10 best linear predictors are included in the multiple regression predictor search.	Allowable values are 1st day of any calendar month.
User	Choose the number of linear predictors from each list, which are to contribute to the multiple regression predictor search.	Option is 1 to 10. Default is 5.
User	Define any exclusions for grouping of predictors in multiple regression predictor search.	Use all or any combination of defined predictors. Typical exclusions are: - use one of MSLP or H1000 but not both - use one of H700 or H500 but not both - use one of D700 or D500 but not both.
Automatic	Execute all possible multiple regression tests using allowable combinations of selected predictors. Construct and store lists of the 50 best multiple regression equations as determined by values of the Composite Skill Index (CSI).	
User	Select up to 3 equations from the 50 best list for operational use.	

3. GEOGRAPHICAL DOMAIN FOR METEOROLOGICAL PREDICTORS IN THE BEAUFORT SEA REGION

Previous east coast work (Davidson, 1992) has shown that variations in the choice of the geographical domain for calculation of eigenfunctions, and hence for selection of predictors, can have significant effects on the level of hindcast skill obtained. Determination of the sensitivity of hindcast results in Beaufort Sea long range ice prediction, to the boundaries of the predictor domain, was one objective of the present work. Thorough investigations have been undertaken to assess the effect of predictor domain variability in the Beaufort Sea region, using eight different predictor domains, defined as follows:

Region Name	Latitude Range	Longitude Range
7 x 7	60° - 90° N	110° - 170° W
8 x 8	55° - 90° N	100° - 170° W
9 x 9	50° - 90° N	100° - 180° W
10 x 10 E (east)	45° - 90° N	90° - 180° W
10 x 10 C (centre)	45° - 90° N	120° - 210° W
10 x 10 W (west)	45° - 90° N	180° - 270° W
11 x 11	40° - 90° N	80° - 180° W
12 x 12	35° - 90° N	80° - 180° W

The locations of the first four of these regions (7 x 7, 8 x 8, 9 x 9, 10 x 10 E) are illustrated in Figure 3.1, while Figure 3.2 shows the locations of the three 10 x 10 regions. Regions 11 x 11 and 12 x 12 are not displayed, but are defined in the table above. Meteorological predictor data are organized on grids spanning these regions, with data values available at 5° latitude and 10° longitude spacing. All grids have redundant values for each longitude at latitude 90°N.

Full sets of linear and multiple regression tests were undertaken for each of these regions, and the highest ranked multiple regression equations were retained for each region, for one month sea ice area prediction, commencing on each of July 1, August 1, and September 1. In this evaluation, such equations are referred to as "Best" equations, associated with a particular region and issue date. These equations were then employed to assess predictor region variations in two manners. Firstly, the equations were employed directly, and the hindcast skill results between regions were compared for each issue date. In this configuration, the Best 7 x 7 equation was used to produce hindcast results for the 7 x 7 region, the Best 8 x 8 equation was employed to produce hindcast results for the 8 x 8 region, and so on. Results of this comparison, for the months July, August, and September appear in the three panels of Table 3.1. If there is a predictor region which has significant advantage in yielding skilful hindcasts, it should be conspicuous in such a comparison. Similarly, regions yielding particularly poor hindcast results

Figure 3.1 Selected Geographical Domains Used to Test Predictors in the Beaufort Sea Region

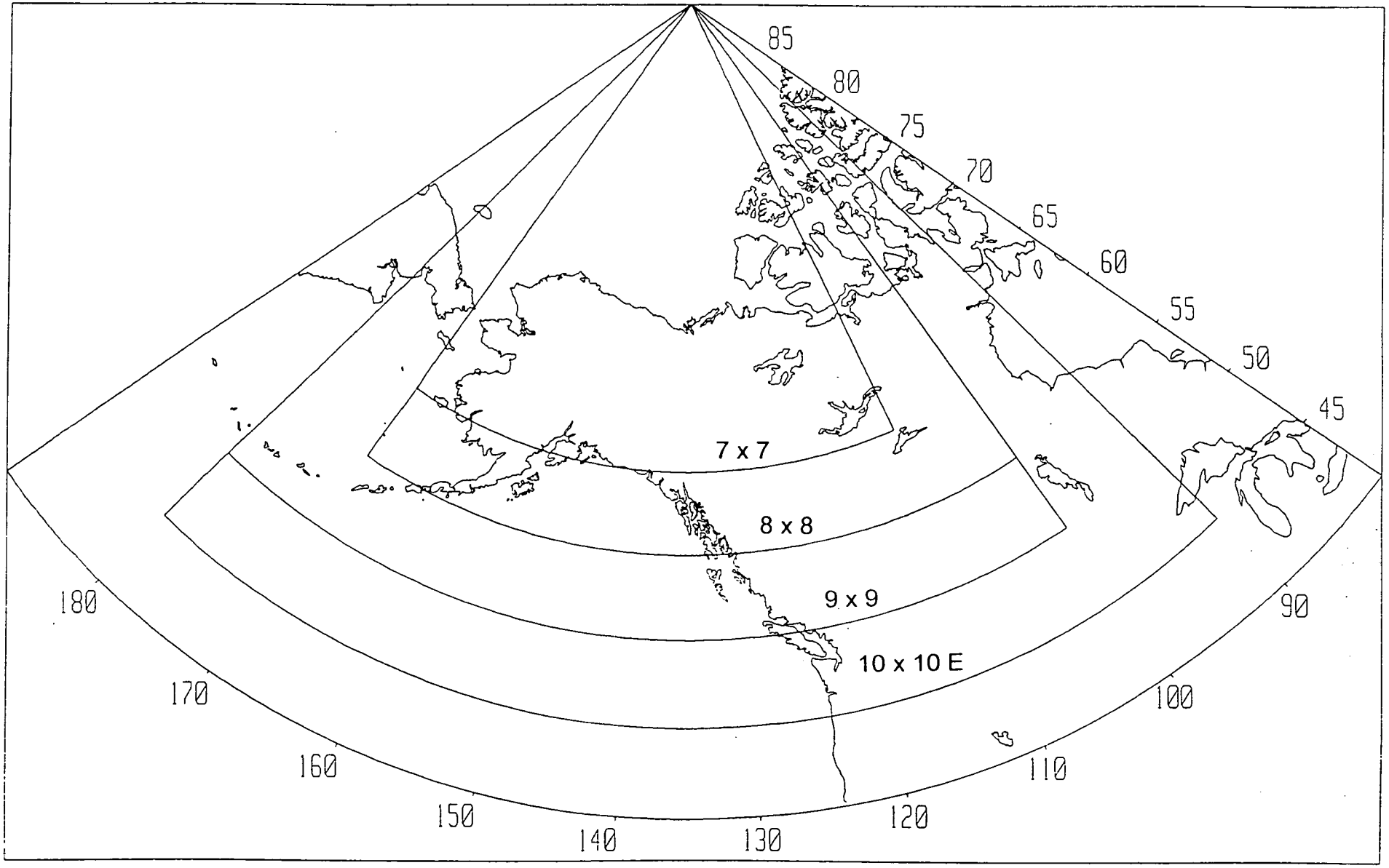

Figure 3.2 Boundaries of Three 10 x 10 Geographical Predictor Regions

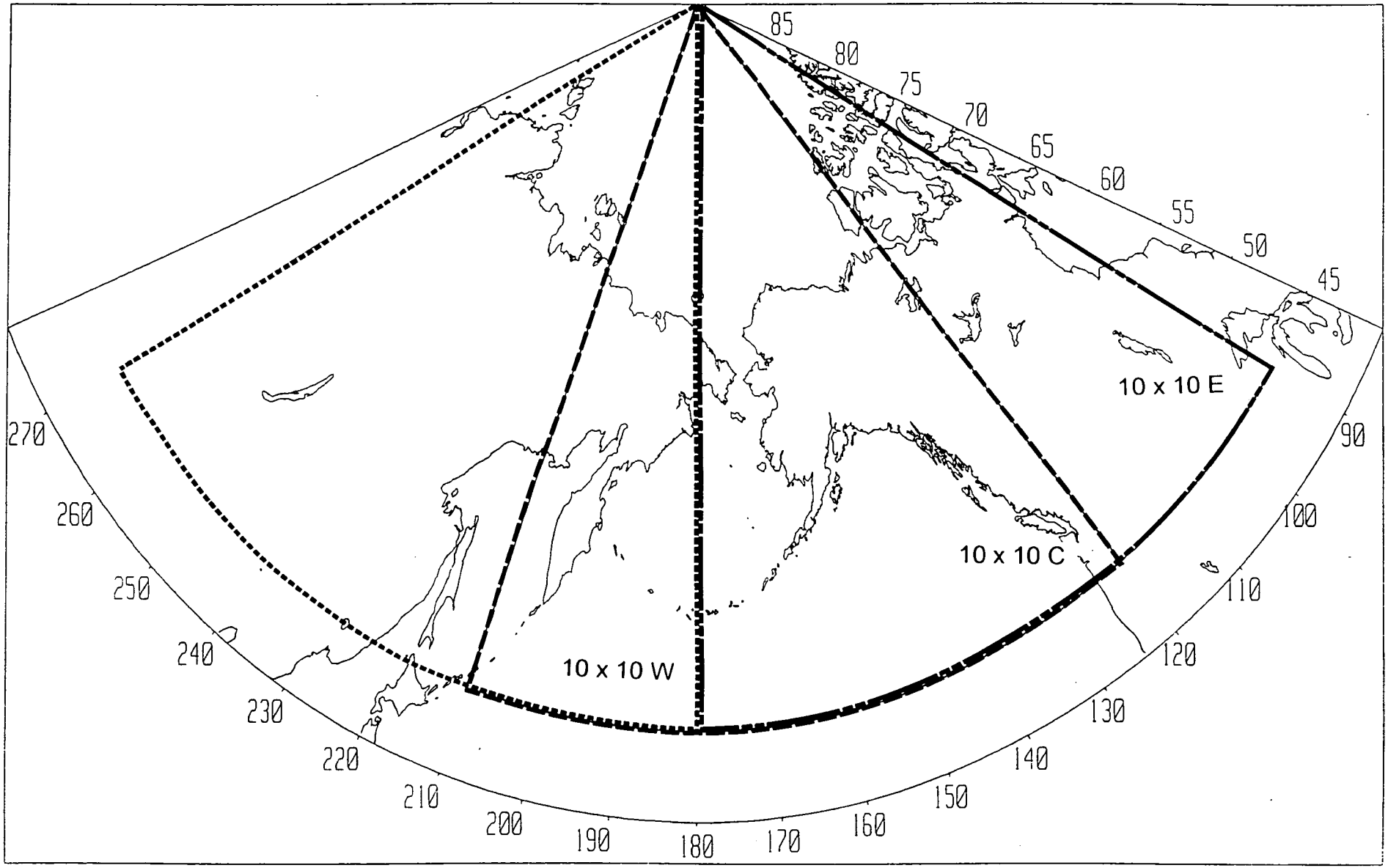

should be easily discriminated. In a second type of evaluation, the Best equations as defined above were used to execute hindcasts across all regions. That is , each Best equation was used as the basis for executing a hindcast in each of eight regions. The results are summarized in Table 3.2 for July issue date, Table 3.3 for August issue date, and Table 3.4 for September issue date. Each of these three tables summarizes hindcast results for as many non-redundant Best equations as were available. Redundant equations result, for example, if say the Best 7 x 7 equation employs exactly the same parameters and eigenfunction coefficients as does the Best 11 x 11 equation for a particular issue date. If hindcasts are particularly sensitive to region, the expected behaviour in this type of test should be that the region matched to the equation will produce significantly better hindcast results than will any region not matched to the equation.

Incorporating information from each of the July, August and September tests summarized in Table 3.1, two generalized conclusions are possible. Firstly, it is abundantly clear that the 10 x 10 W predictor region (centred over Siberia) is not appropriate for use in Beaufort Sea long range prediction. The July CSI value for 10 x 10 W is only half the magnitude of its counterparts for 10 x 10 E and 10 x 10 C. Similarly in August, the 10 x 10 W CSI value drops below its counterparts. Secondly, there appears to be grounds on the basis of September behaviour to discredit use of 12 x 12. Other than these two solid conclusions, it is noted that 7 x 7 consistently performs well, and that each of 7 x 7 through 11 x 11 appears to perform adequately. The 10 x 10 W region centred over the Beaufort Sea itself marginally outperforms the 10 x 10 C region which is displaced 30 longitudinal degrees to the west.

These conclusions are endorsed by the results appearing in Tables 3.2 through 3.4 The 10 x 10 W region is not usable, and the 10 x 10 E is consistently preferred over the corresponding 10 x 10 C. The 12 x 12 is less attractive in most situations that the smaller regions, and particularly returns poor hindcast results for September, as demonstrated in the bottom panel in Figure 3.4.

It appears on the basis of these investigations, that the Beaufort Sea ice area hindcasts are largely insensitive to geographical predictor region for the range of regions defined and aligned here as 7 x 7, 8 x 8, 9 x 9, 10 x 10 E and 11 x 11 (see Figure 3.1). Use of any of these regions as a base from which to search for viable multiple regression equations is well justified. The operational version of LRIFS now installed at Ice Centre, Ottawa, makes it very simple to undertake further investigations of this nature. In Chapter 4.6 of this report, operational equations based on the 10 x 10 E region are identified. Other operational equations can similarly be defined with little difficulty from any of 7 x 7, 8 x 8, 9 x 9 or 11 x 11.

Table 3.1 Effect of Geographical Variation While Using Best Equation Source Matched to Each Region

Ice Signal: 1 mos July

Equation Source	Geographical Region	"r"	"CSI"	Category Error 0	1	2	Class Error 0	1	2	3	4	Delta Rank Most Severe Cases 5	4	3	2	1
Best 7 x 7	7 x 7	0.82	0.86	13	8	0	8	12	1			-1	2	-1	-1	0
Best 8 x 8	8 x 8	0.78	0.83	11	10	0	11	9	1			-2	1	1	-2	0
Best 9 x 9	9 x 9	0.76	0.80	13	8	0	9	11	1			-5	1	1	-2	0
Best 10 x 10 E	10 x 10 E	0.73	0.82	13	8	0	12	7	2			-1	1	1	-3	0
Best 11 x 11	11 x 11	0.72	0.77	11	10	0	9	10	2			-1	2	0	-5	0
Best 12 x 12	12 x 12	0.72	0.76	11	10	0	9	10	2			-2	2	0	-4	0
Best 10 x 10 E	10 x 10 E	0.73	0.82	13	8	0	12	7	2			-1	1	1	-3	0
Best 10 x 10 C	10 x 10 C	0.75	0.80	13	8	0	11	9	1			-2	2	0	-3	0
Best 10 x 10 W	10 x 10 W	0.47	0.43	6	12	3	9	8	4			-5	3	-3	-7	1

Ice Signal: 1 mos August

Equation Source	Geographical Region	"r"	"CSI"	Category Error 0	1	2	Class Error 0	1	2	3	4	Delta Rank Most Severe Cases 5	4	3	2	1
Best 7 x 7	7 x 7	0.92	0.93	15	6	0	12	9				-1	0	0	1	-1
Best 8 x 8	8 x 8	0.86	0.84	15	6	0	8	13				-2	2	0	1	-4
Best 9 x 9	9 x 9	0.82	0.88	15	6	0	9	12				0	0	1	1	-2
Best 10 x 10 E	10 x 10 E	0.77	0.85	13	8	0	8	13				1	-1	1	1	-2
Best 12 x 12	12 x 12	0.85	0.85	13	8	0	9	12				-2	1	1	1	-3
Best 10 x 10 E	10 x 10 E	0.77	0.85	13	8	0	8	13				1	-1	1	1	-2
Best 10 x 10 C	10 x 10 C	0.76	0.80	11	10	0	7	13	1			0	1	1	1	-6
Best 10 x 10 W	10 x 10 W	0.63	0.70	10	10	1	4	15	2			0	-2	0	1	-3

Ice Signal: 1 mos September

Equation Source	Geographical Region	"r"	"CSI"	Category Error 0	1	2	Class Error 0	1	2	3	4	Delta Rank Most Severe Cases 5	4	3	2	1
Best 7 x 7	7 x 7	0.83	0.83	17	4	0	12	9				3	-1	2	-1	-5
Best 8 x 8	8 x 8	0.69	0.76	11	10	0	6	12	3			0	-3	1	1	-2
Best 9 x 9	9 x 9	0.74	0.79	15	6	0	11	6	4			2	0	1	1	-4
Best 10 x 10 E	10 x 10 E	0.79	0.84	15	6	0	10	9	2			1	-2	1	1	-2
Best 11 x 11	11 x 11	0.76	0.79	11	10	0	9	10	2			2	-4	-1	1	-1
Best 12 x 12	12 x 12	0.38	0.40	9	10	2	8	9	4			1	-5	-13	1	-7

Table 3.2 Effects of Geographical Variation for July Hindcasts, While Using Equation Sources Which Are Not Matched to Each Region

Ice Signal: 1 mos July

Equation Source	Geographical Region	"r"	"CSI"	Category Error 0	1	2	Class Error 0	1	2	3	4	Delta Rank Most Severe Cases 5	4	3	2	1
Best 7 x 7	7 x 7	0.82	0.86	13	8	0	8	12	1			-1	2	-1	-1	0
	8 x 8	0.78	0.79	11	10	0	9	10	2			-2	2	0	-3	0
	9 x 9	0.78	0.78	0	1	2	8	11	2			-2	2	0	-4	0
	10 x 10 E	0.76	0.77	11	10	0	8	11	2			-2	2	0	-4	0
	11 x 11	0.72	0.77	11	10	0	9	10	2			-1	2	0	-5	0
	12 x 12	0.72	0.76	11	10	0	9	10	2			-2	2	0	-4	0
Best 7 x 7	10 x 10 E	0.76	0.77	11	10	0	8	11	2			-2	2	0	-4	0
	10 x 10 C	0.75	0.80	13	8	0	11	9	1			-2	2	0	-3	0
	10 x 10 W	0.47	0.43	6	12	3	9	8	4			-5	3	-3	-7	-1

Equation Source	Geographical Region	"r"	"CSI"	Category Error 0	1	2	Class Error 0	1	2	3	4	Delta Rank Most Severe Cases 5	4	3	2	1
Best 8 x 8	7 x 7	0.81	0.87	11	10	0	11	9	1			-1	-1	1	-1	0
	8 x 8	0.78	0.83	11	10	0	11	9	1			-2	1	1	-2	0
	9 x 9	0.76	0.82	13	8	0	11	9	1			-2	1	1	-3	0
	10 x 10 E	0.75	0.81	13	8	0	11	9	1			-2	1	1	-3	0
	11 x 11	0.73	0.80	13	8	0	9	11	1			-2	0	1	-3	0
	12 x 12	0.72	0.79	13	8	0	9	10	2			-2	1	1	-3	0

Table 3.2 (cont.)

Equation Source	Geographical Region	"r"	"CSI"	Category Error 0	1	2	Class Error 0	1	2	3	4	Delta Rank Most Severe Cases 5	4	3	2	1
Best 9 x 9	7 x 7	0.73	0.75	12	8	1	9	11	1			-3	2	0	-2	0
	8 x 8	0.75	0.81	13	8	0	9	11	1			-4	1	1	-2	0
	9 x 9	0.76	0.80	13	8	0	9	11	1			-5	1	1	-2	0
	10 x 10 E	0.75	0.76	11	10	0	8	12	1			-5	2	0	-3	0
	11 x 11	0.73	0.77	11	10	0	7	13	1			-4	1	1	-3	0
	12 x 12	0.73	0.75	11	10	0	8	12	1			-5	2	0	-3	0

Equation Source	Geographical Region	"r"	"CSI"	Category Error 0	1	2	Class Error 0	1	2	3	4	Delta Rank Most Severe Cases 5	4	3	2	1
Best 10 x 10 E	7 x 7	0.73	0.78	12	8	1	11	9	1			-1	1	1	-3	0
	8 x 8	0.74	0.83	13	8	0	11	9	1			-1	1	1	-3	0
	9 x 9	0.73	0.83	13	8	0	12	8	1			-1	1	1	-3	0
	10 x 10 E	0.73	0.82	13	8	0	12	7	2			-1	1	1	-3	0
	11 x 11	0.73	0.82	13	8	0	13	6	2			-1	0	1	-3	0
	12 x 12	0.73	0.82	13	8	0	13	6	2			-1	0	1	-3	0
Best 10 x 10 E	10 x 10 E	0.73	0.82	13	8	0	12	7	2			-1	1	1	-3	0
	10 x 10 C	0.68	0.63	13	6	2	10	9	2			-2	1	1	-3	0
	10 x 10 W	0.50	0.50	10	6	5	12	6	3			-6	0	1	-8	0

Table 3.3 Effects of Geographical Variation for August Hindcasts, While Using Equation Sources Which Are Not Matched to Each Region

Ice Signal: 1 mos August

Equation Source	Geographical Region	"r"	"CSI"	Category Error 0	1	2	Class Error 0	1	2	3	4	Delta Rank Most Severe Cases 5	4	3	2	1
Best 7 x 7	7 x 7	0.92	0.93	15	6	0	12	9				-1	0	0	1	-1
	8 x 8	0.70	0.64	13	6	2	10	9	2			2	-1	1	1	-3
	9 x 9	0.68	0.59	12	6	3	10	9	2			2	0	2	0	-5
	10 x 10 E	0.65	0.56	12	6	3	9	10	2			2	-2	2	0	-6
	11 x 11	0.65	0.55	12	6	3	8	11	2			2	-3	2	0	-5
	12 x 12	0.65	0.56	12	6	3	7	12	2			2	-2	2	0	-6

Equation Source	Geographical Region	"r"	"CSI"	Category Error 0	1	2	Class Error 0	1	2	3	4	Delta Rank Most Severe Cases 5	4	3	2	1
Best 8 x 8	7 x 7	0.86	0.83	13	8	0	7	14				-2	2	0	1	-4
	8 x 8	0.86	0.84	15	6	0	8	13				-2	2	0	1	-4
	9 x 9	0.86	0.85	15	6	0	8	13				-2	1	1	1	-4
	10 x 10 E	0.85	0.84	13	8	0	8	13				-2	1	1	1	-4
	11 x 11	0.84	0.84	13	8	0	8	13				-2	1	1	1	-4
	12 x 12	0.85	0.84	13	8	0	8	13				-2	1	1	1	-4

Equation Source	Geographical Region	"r"	"CSI"	Category Error 0	1	2	Class Error 0	1	2	3	4	Delta Rank Most Severe Cases 5	4	3	2	1
Best 9 x 9	7 x 7	0.86	0.85	13	8	0	12	9				2	0	1	1	-4
	8 x 8	0.82	0.84	13	8	0	9	12				2	-1	1	1	-3
	9 x 9	0.82	0.88	15	6	0	9	12				0	0	1	1	-2
	10 x 10 E	0.79	0.82	13	8	0	8	13				2	-2	1	1	-3
	11 x 11	0.77	0.77	11	10	0	8	12	1			2	-4	1	1	-3
	12 x 12	0.76	0.77	11	10	0	8	12	1			2	-4	1	1	-3

Table 3.3 (cont.)

Equation Source	Geographical Region	"r"	"CSI"	Category Error 0	1	2	Class Error 0	1	2	3	4	Delta Rank Most Severe Cases 5	4	3	2	1
Best 10 x 10 E	7 x 7	0.82	0.73	15	4	2	11	10				-1	0	1	1	-2
	8 x 8	0.79	0.83	14	6	1	11	10				-1	0	1	1	-2
	9 x 9	0.80	0.83	14	6	1	9	12				-1	0	1	1	-2
	10 x 10 E	0.77	0.85	13	8	0	8	13				1	-1	1	1	-2
	11 x 11	0.75	0.79	13	8	0	9	11	1			2	-2	1	1	-3
	12 x 12	0.74	0.78	13	8	0	8	11	2			2	-2	1	1	-3

Equation Source	Geographical Region	"r"	"CSI"	Category Error 0	1	2	Class Error 0	1	2	3	4	Delta Rank Most Severe Cases 5	4	3	2	1
Best 10 x 10 E	10 x 10 E	0.77	0.85	13	8	0	8	13				1	-1	1	1	-2
	10 x 10 C	0.73	0.76	11	10	0	8	11	2			-2	-4	1	1	-2
	10 x 10 W	0.48	0.47	11	6	4	5	14	2			-1	-13	1	1	-8
Best 10 x 10 C	10 x 10 E	0.79	0.82	13	8	0	9	11	1			0	1	1	1	-6
	10 x 10 C	0.76	0.80	11	10	0	7	13	1			0	1	1	1	-6
	10 x 10 W	0.61	0.67	8	12	1	5	14	2			2	-1	1	1	-7
Best 10 x 10 W	10 x 10 E	0.75	0.75	11	10	0	8	12	1			-2	2	0	1	-9
	10 x 10 C	0.73	0.68	8	12	1	6	14	1			-3	2	0	1	-8
	10 x 10 W	0.63	0.70	10	10	1	4	15	2			0	-2	0	1	-3

Equation Source	Geographical Region	"r"	"CSI"	Category Error 0	1	2	Class Error 0	1	2	3	4	Delta Rank Most Severe Cases 5	4	3	2	1
Best 12 x 12	7 x 7	0.87	0.84	13	8	0	9	12				-2	2	0	1	-3
	8 x 8	0.86	0.81	11	10	0	10	11				-3	2	0	1	-4
	9 x 9	0.86	0.86	13	8	0	10	11				-2	1	1	1	-3
	10 x 10 E	0.85	0.85	13	8	0	10	11				-2	1	1	1	-4
	11 x 11	0.85	0.83	13	8	0	9	12				-2	2	0	1	-4
	12 x 12	0.85	0.85	13	8	0	9	12				-2	1	1	1	-3

Table 3.4 Effects of Geographical Variation for September Hindcasts, While Using Equation Sources Which Are Not Matched to Each Region

Ice Signal: 1 mos September

Equation Source	Geographical Region	"r"	"CSI"	Category Error 0	1	2	Class Error 0	1	2	3	4	Delta Rank Most Severe Cases 5	4	3	2	1
Best 7 x 7	7 x 7	0.83	0.83	17	4	0	12	9				3	-1	2	-1	-5
	8 x 8	0.72	0.71	15	6	0	12	5	4			3	-7	2	-1	-3
	9 x 9	0.69	0.69	15	6	0	10	8	3			3	-10	2	-1	-4
	10 x 10 E	0.69	0.64	12	8	1	11	7	3			3	-9	2	-1	-5
	11 x 11	0.64	0.61	10	10	1	9	8	4			2	-9	2	0	-6
	12 x 12	0.63	0.60	10	10	1	10	7	4			2	-9	2	0	-7

Equation Source	Geographical Region	"r"	"CSI"	Category Error 0	1	2	Class Error 0	1	2	3	4	Delta Rank Most Severe Cases 5	4	3	2	1
Best 8 x 8	7 x 7	0.70	0.74	11	10	0	7	11	3			2	-3	1	1	-3
	8 x 8	0.69	0.76	11	10	0	6	12	3			0	-3	1	1	-2
	9 x 9	0.67	0.70	10	10	1	6	12	3			-1	-5	1	1	-2
	10 x 10 E	0.64	0.65	10	10	1	7	11	3			-4	-3	1	1	-3
	11 x 11	0.62	0.54	9	10	2	7	11	3			-6	-2	1	1	-3
	12 x 12	0.61	0.54	9	10	2	8	10	3			-6	-2	1	1	-3

Equation Source	Geographical Region	"r"	"CSI"	Category Error 0	1	2	Class Error 0	1	2	3	4	Delta Rank Most Severe Cases 5	4	3	2	1
Best 9 x 9	7 x 7	0.69	0.58	11	8	2	9	10	2			4	0	1	-1	-7
	8 x 8	0.71	0.76	13	8	0	9	9	3			2	0	2	0	-4
	9 x 9	0.74	0.79	15	6	0	11	6	4			2	0	1	1	-4
	10 x 10 E	0.74	0.78	13	8	0	9	8	4			2	-1	1	1	-3
	11 x 11	0.70	0.70	12	8	1	9	8	4			3	-2	0	1	-3
	12 x 12	0.70	0.70	12	8	1	9	8	4			3	-2	0	1	-3

Table 3.4 (cont.)

Source	Geographical Region	"r"	"CSI"	Category Error 0	1	2	Class Error 0	1	2	3	4	Delta Rank Most Severe Cases 5	4	3	2	1
Best 10 x 10 E	7 x 7	0.73	0.62	17	2	2	11	7	3			3	-2	2	-1	-3
	8 x 8	0.75	0.75	13	8	0	11	8	2			3	-3	2	-1	-3
	9 x 9	0.79	0.78	14	6	1	9	11	1			2	-1	2	0	-3
	10 x 10 E	0.79	0.84	15	6	0	10	9	2			1	-2	1	1	-2
	11 x 11	0.74	0.73	12	8	1	10	8	3			1	-6	1	1	-2
	12 x 12	0.74	0.73	12	8	1	10	8	3			1	-6	1	1	-2

Equation Source	Geographical Region	"r"	"CSI"	Category Error 0	1	2	Class Error 0	1	2	3	4	Delta Rank Most Severe Cases 5	4	3	2	1
Best 11 x 11	7 x 7	0.69	0.58	13	6	2	9	10	2			4	0	1	-1	-10
	8 x 8	0.76	0.77	15	6	0	10	9	2			3	-1	2	-1	-6
	9 x 9	0.78	0.79	15	6	0	11	7	3			3	0	0	1	-5
	10 x 10 E	0.77	0.77	13	8	0	10	8	3			3	-2	0	1	-3
	11 x 11	0.76	0.79	11	10	0	9	10	2			2	-4	-1	1	-1
	12 x 12	0.77	0.78	11	10	0	9	10	2			2	-5	-1	1	-1

Equation Source	Geographical Region	"r"	"CSI"	Category Error 0	1	2	Class Error 0	1	2	3	4	Delta Rank Most Severe Cases 5	4	3	2	1
Best 12 x 12	7 x 7	0.28	0.39	8	12	1	8	7	6			-8	2	-5	-7	-6
	8 x 8	0.33	0.47	10	10	1	8	8	5			-5	1	-9	-3	-5
	9 x 9	0.30	0.37	7	12	2	7	9	5			-2	-2	-12	-1	-8
	10 x 10 E	0.31	0.36	10	8	3	8	8	5			-2	-6	-14	0	-5
	11 x 11	0.35	0.38	8	10	3	8	8	5			1	-5	-13	-1	-9
	12 x 12	0.38	0.40	9	10	2	8	9	4			1	-5	-13	1	-7

4. LONG-RANGE PREDICTION OF BEAUFORT SEA ICE SEASON SEVERITY

4.1 Beaufort Sea Ice Area Severity Index

A single ice area index has been employed in this work to characterize Beaufort Sea ice occurrence severity. This index has been developed from digital versions of AES Beaufort Sea area ice charts for the years 1960 to 1980.

These charts characterize ice abundance in the region from the North American mainland coast, at about 68° N, northward to 75° N latitude. These ice charts span a longitudinal swath extending from 120° to 160° W longitude.

Digital sea ice data acquired from AES occupy a 1.0° longitude by 0.25° latitude grid. Grids exist weekly through the sea ice season in the region, but in the initial form, the data are interrupted with many gaps in both time and space.

In preparation for calculating ice indices from this data set it was necessary to establish data continuity in both time and space. Temporal averages were not problematic, because weekly concentration values were arithmetically averaged to yield monthly ice grids. Missing weeks posed little problem, as the appropriate average was simply calculated using three rather than four weeks. There was no case encountered where these data gaps prohibited calculation of reasonable mean grid values for each calendar month.

Spatial interpolation for missing grid values of ice concentration was accomplished using two schemes. Persistence was used as a first method, wherever possible, by filling a single missing grid concentration value with its counterpart from the preceding week. For time gaps greater then one week in a given concentration value at a given grid point, it was elected to use monthly mean values calculated across all available observations at that grid point to fill the second and subsequent missing weeks.

In preparation for calculating ice area indices, values of sea surface area for each cell of the sea ice data grid were also prepared. For coastal grid elements containing any land area, the subsection of the grid cell representing sea surface was estimated.

Ice Area Index values are the summation of the ice area which exists in each grid cell of the region over the desired time interval. The total ice concentration for a grid point is converted to its corresponding ice area value by multiplying with the area of sea surface pertinent to in the cell. The set of grids which constitute a month are then averaged, producing a single mean area grid for each month. The set of monthly area grids are then averaged over the desired number of months. All of the grid values which constitute a month are then totalled to produce the desired ice area index.

Experience with EOF forecasting methods indicates that the highest skill is achieved when attempting to predict an ice index series which has high variability. If there is particularly low variability in the predictand series, the multiple regression models tend to degenerate to predicting a near constant value, and mistakenly then appear to be somewhat skilful. In such

cases, the multiple regression models loose sensitivity to their composition of predictors, and any one group of predictors fares almost as well as any other. No true skill is really achieved, because the signal being predicted has little variability in the first place.

The annual cycle of sea ice occurrence in the Beaufort Sea is such that some months could demonstrate such low variability as to disqualify them from investigation with LRIFS. The ice season is dominated by a long, winter season with near 100% ice cover, and virtually no variability. Study of the available AES ice data confirms that this situation persists between November and May in all years. The annual break-up of the southern Beaufort Sea pack can commence in June, and the pack then retreats northward through July and August. The onset of the winter ice season can commence as early as September, and certainly is well advanced by the end of October in all years. Thus, the months with measurable variability in ice cover extend from June to October, with both this first and last months likely to demonstrate less flucuation in ice conditions than the summer months of July, August and September.

The ice index series employed in this work are graphically demonstrated in Figures 4.1(a) and 4.1(b). In the first panel (Figure 4.1(a)), monthly series for June, July, August and September appear. In the second panel (Figure 4.1(b)) appears the corresponding monthly series for October, plus the three month averages for intervals ending in August, September, and October. These series are linked with the choice of issue dates and valid dates as described in Chapter 4.3 below. In each case, these illustrated series are sorted in ascending order to allow easy assessment of the range of values present in the data. Thus, each graph represents a different time sequence. The important observation is that the range of ice index values is suitably large in all but possibly the June case, to justify the use of these series as predictands in the LRIFS system. Variability is sufficiently low in June that the ablility to predict might be restricted, simply by the nature of the predictand series.

Figure 4.1(a) Beaufort Sea Ice Area Predictand Series
for 1 Month Ending June, July, August, and September

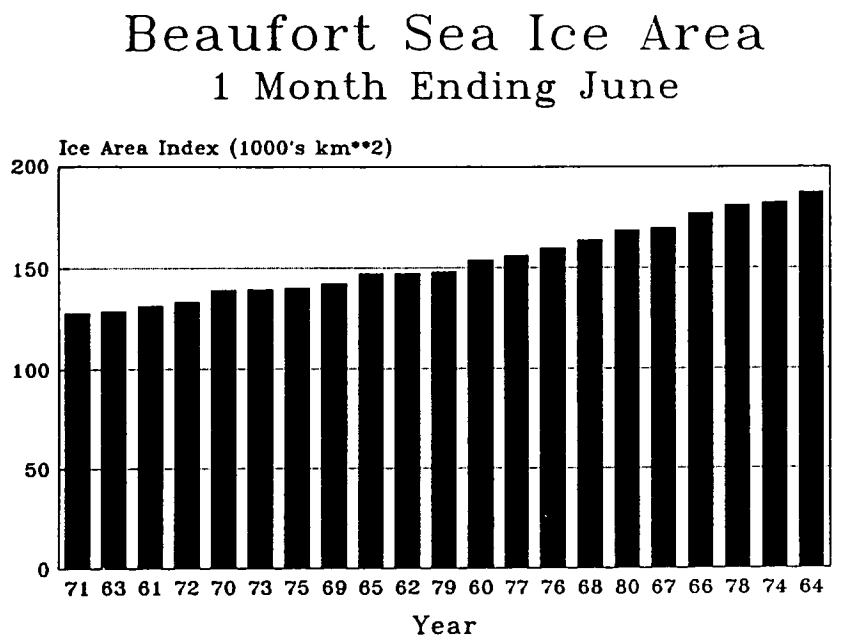

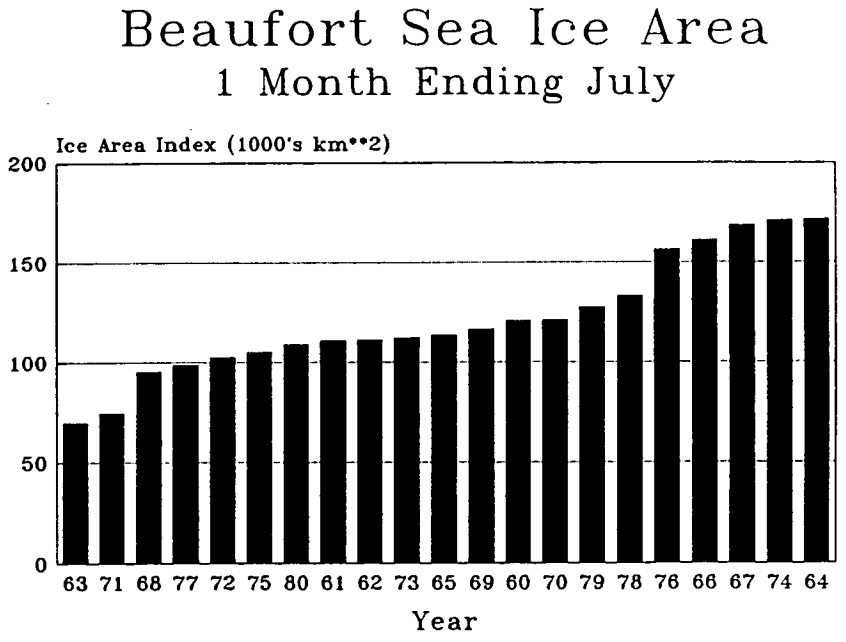

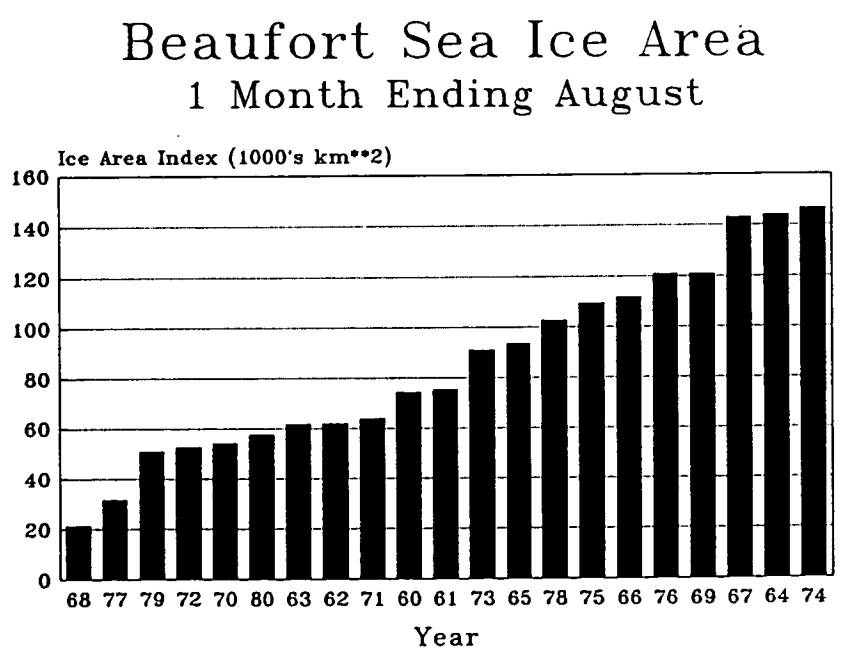

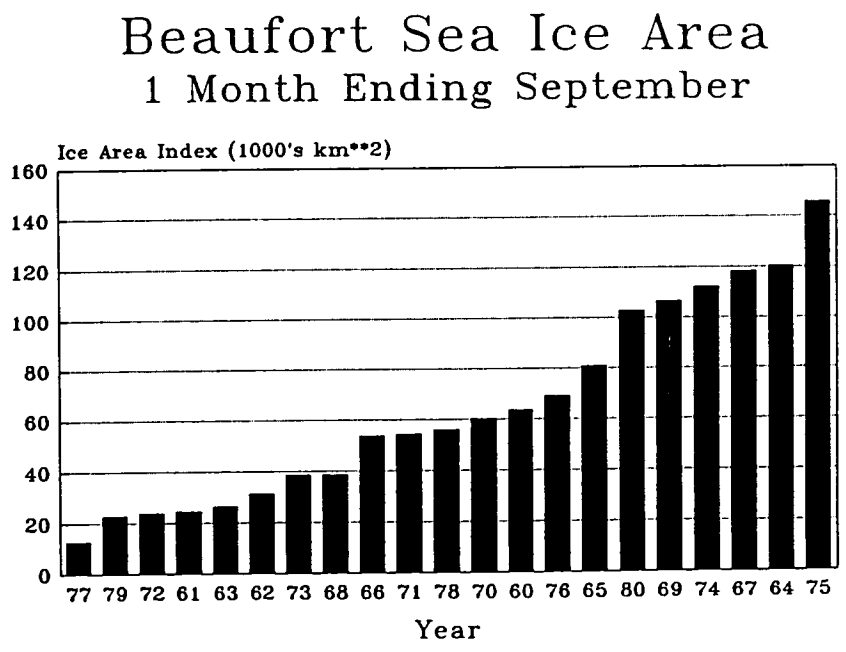

Figure 4.1(b) Beaufort Sea Ice Area Predictand Series
for 1 Month Ending October, and 3 Months Ending August, September, and October

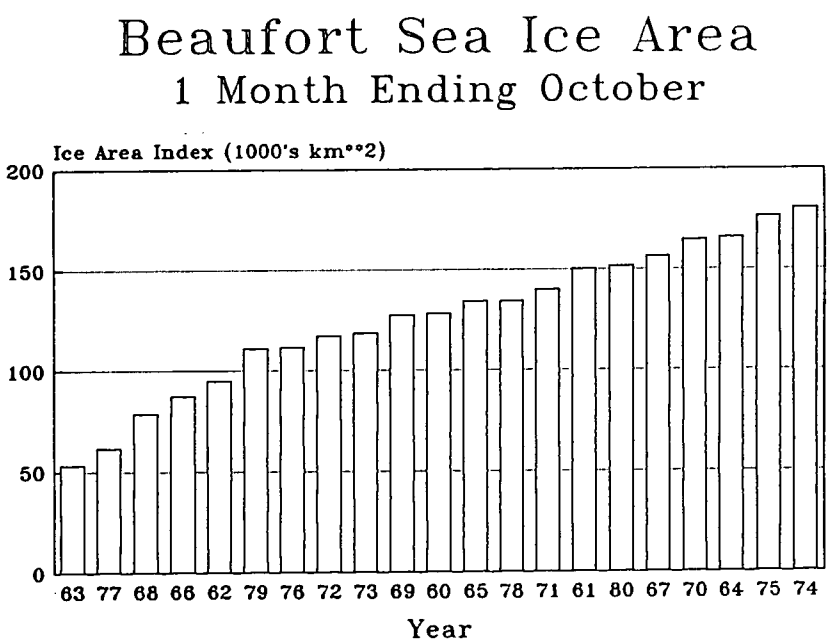

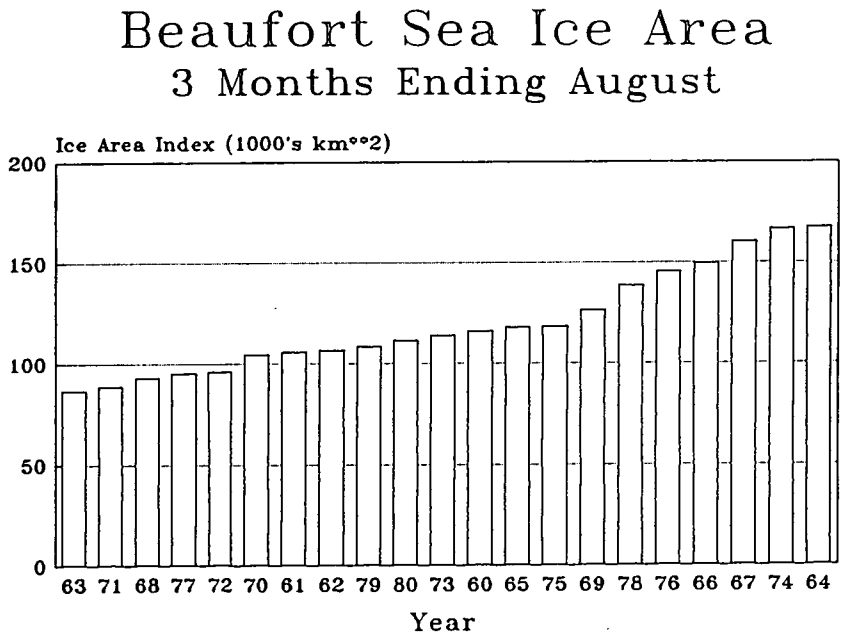

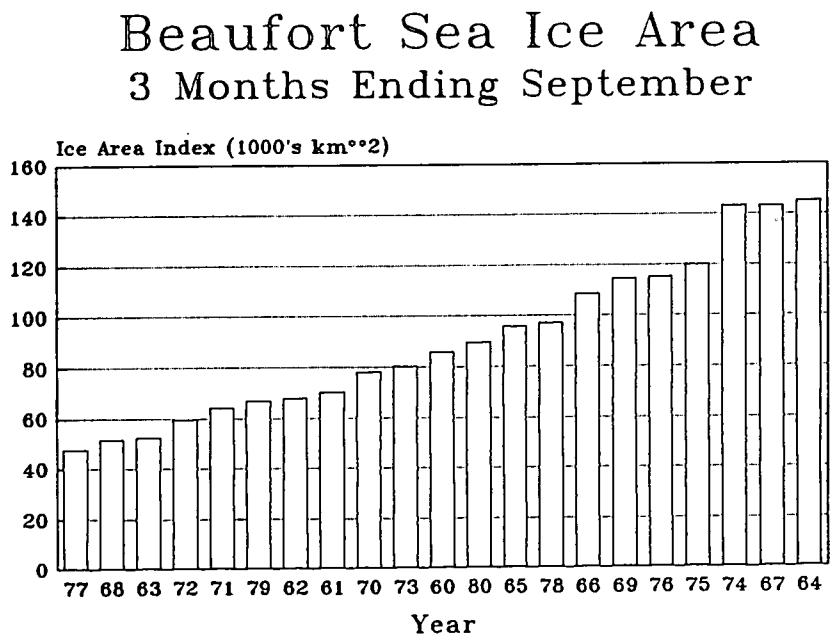

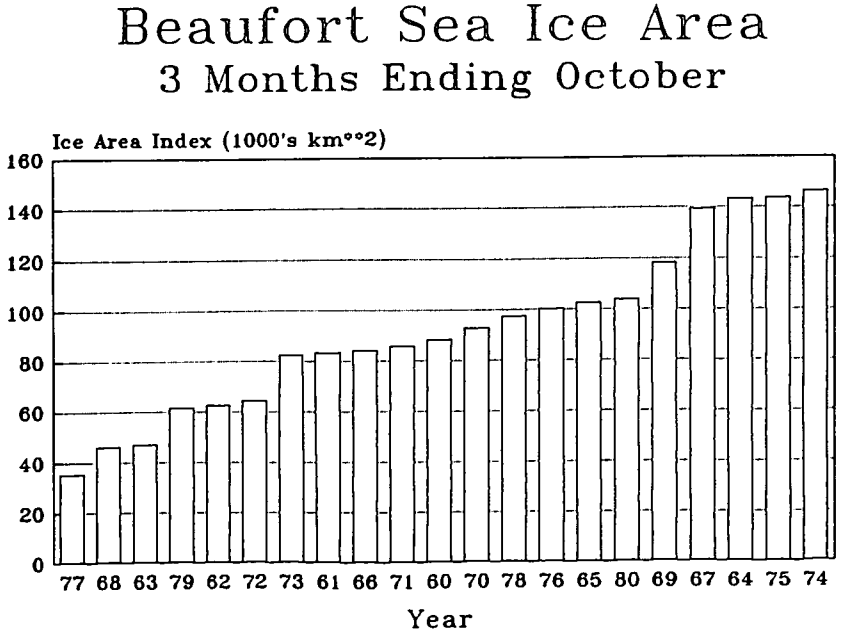

4.2 Meteorological and Ice Predictor Fields

Rather lengthy discussions of the source of meteorological predictor data sets incorporated into LRIFS have been provided previously by Davidson (1987) and Davidson (1992). The three activities undertaken in the present project related to the meteorological predictor data sets include:

- partial reorganization of source data for each parameter, to assemble long time series (1951-1991) with as few concatenations as possible. The guiding principles in assembling these long time series were to employ segments of maximum duration from individual sources, to minimize the number of segments which had to be pieced together to complete the full time series, and to ensure compatibility across all junctions between fragments. These continuity tests included assessment of compatibility of the means of connected segments, and most importantly, compatibility of eigenfunctions between each connected segment.

- addition of a few months of 1991 data which had recently become available, thus extending some parameter data sets beyond the dates which were reported by Davidson (1992).

- expansion of these meteorological source data sets to span the entire northern hemisphere, as described in Chapter 2.3.

- resolution of previously reported problems with the H700 data set (Davidson, 1992).

The present status of meteorological predictor data sets is summarized via Figure 4.2 and Figure 4.3. In the first of these, the individual segments of available data, by original source, are summarized. In the second, the concatenation of individual segments is illustrated to show the present combinations of data sources which are implemented in LRIFS. In this latter Figure 4.3, it is to be noted that the D500 and D700 series have been computed directly by subtracting the H1000 series respectively from the H500 and H700 series which are in current use.

Figure 4.2 Individual Meteorological Data Set Durations and Sources

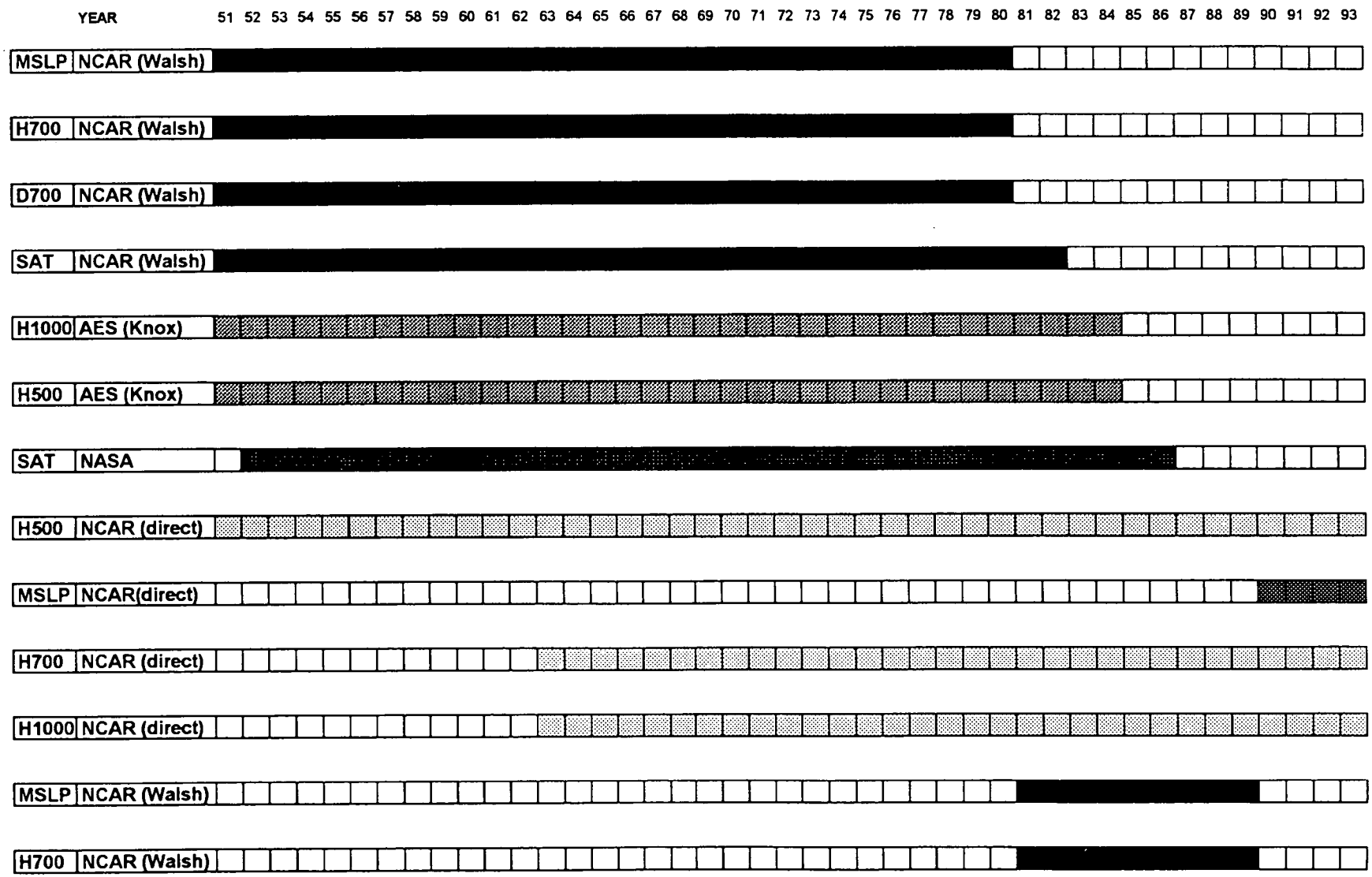

Figure 4.3 Meteorological Data Sets In Use Within LRIFS in Early 1993

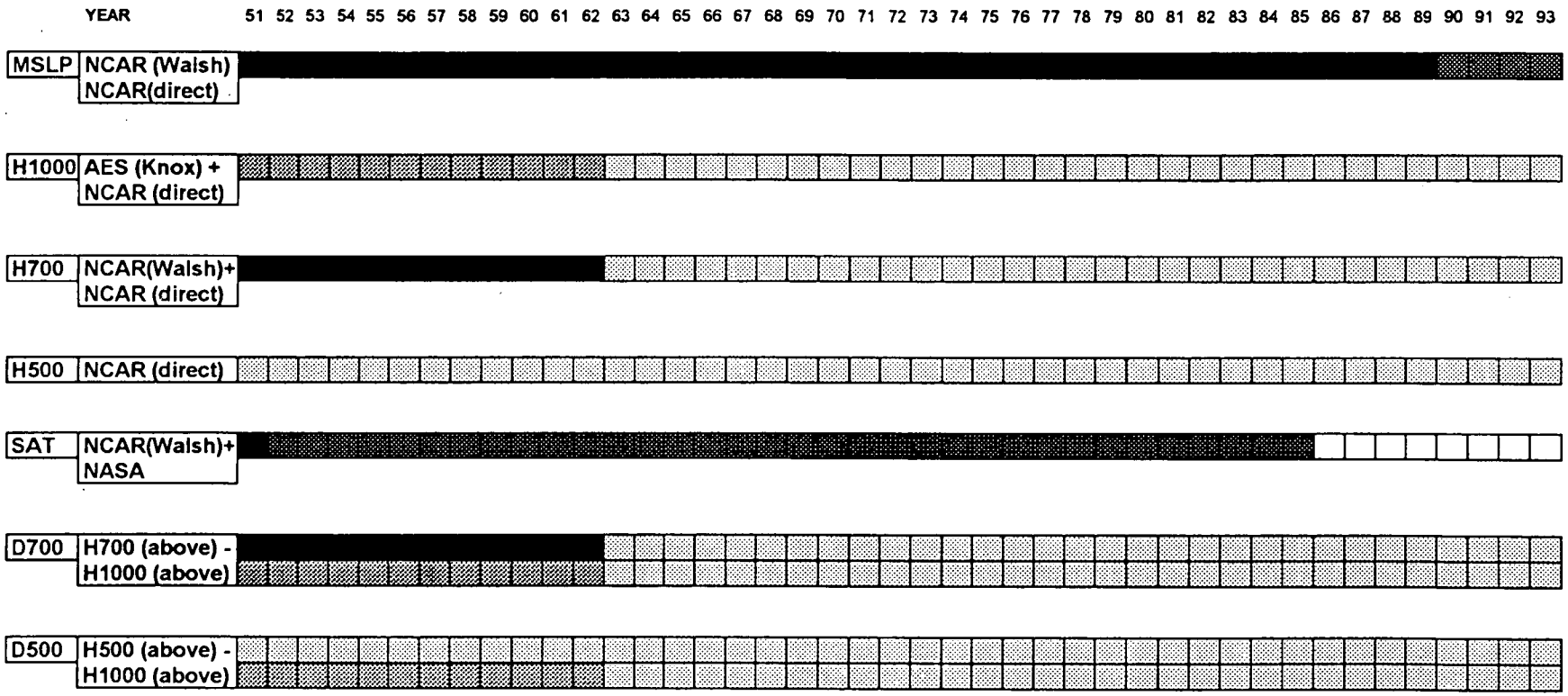

4.3 Definitions of Issue Date and Valid Date

Within LRIFS, allowable "Issue Dates" are aligned on the first of each month, assuming that the corresponding forecast equations make use of predictor data through the last day of the preceding month. For each "Issue Date" in the operational version of LRIFS, forecasts are allowed for one month and three months into the future only. The end points of these allowable forecast intervals are termed "Valid Dates". In the research version of LRIFS (see Pinhorn, 1993b), greater flexibility is offered in the combination of "Issue Dates" and "Valid Dates". The pracitcal set of "Issue Dates" and "Valid Dates" for operational use in the Beaufort Sea, is illustrated in Figure 4.4.

Figure 4.4 Illustration of "Issue Dates" (I) and "Valid Dates"

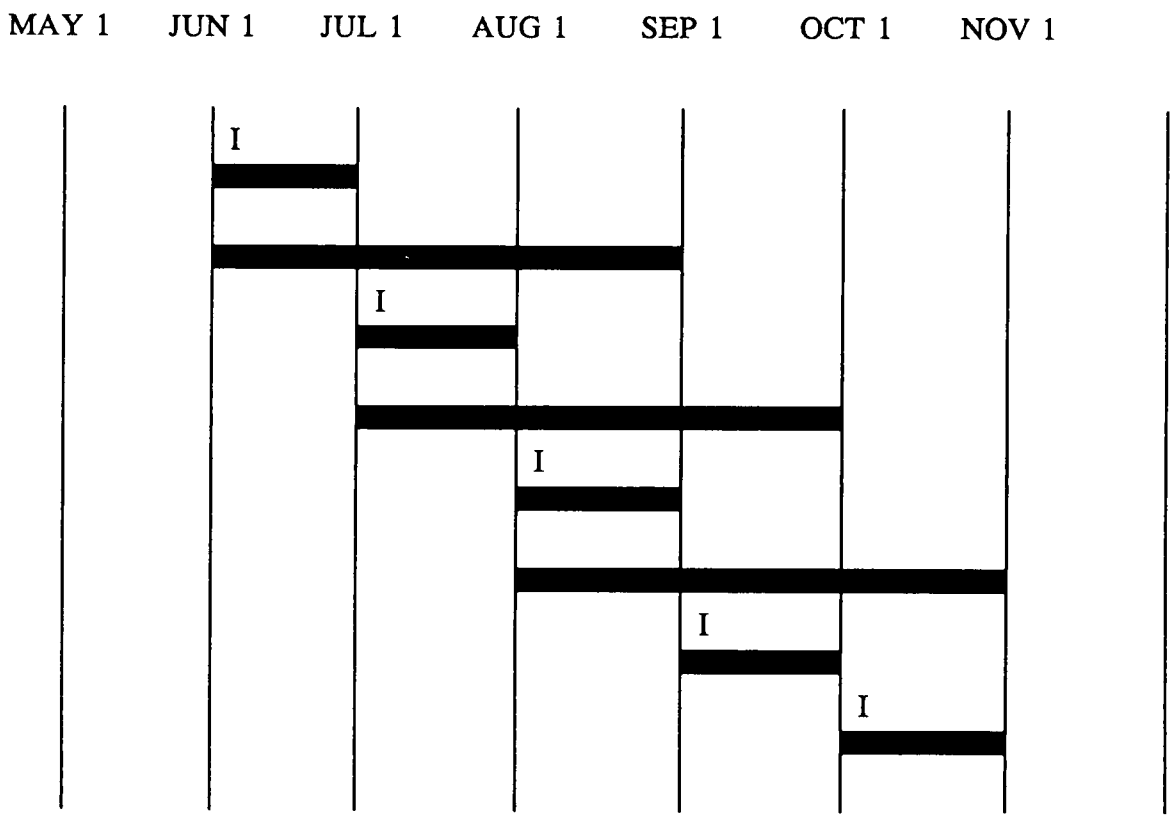

4.4 Antecedent Ice Severity Anomaly as a Predictor

Authors such as Chapman and Walsh (1991) have indicated that antecedent ice severity anomaly alone is a viable predictor of Beaufort Sea ice conditions. The LRIFS system has the capacity to incorporate antecedent ice severity with assorted meteorological predictors in multiple regression combinations. Indeed, the best operational equations (Chapter 4.6) often incorporate ice and meteorological predictors together. It is also instructive to assess the actual strength of the ice predictors, in the absence of meteorological variables. To do so, linear regression models were tested for a series of ice anomaly predictors as described in Table 4.1.

Ice area anomaly values for June through August were employed in various configurations to assess their predictive capacity for ice conditions of one month duration, one to three months later. These results (Table 4.1) clearly identify ice area anomaly as a strong predictor at least one month into the future. The June, July, and August predictions respectively for July, August and September (next immediate month) all return CSI values in excess of 0.7, and at worst return Category Error = 2 values of 2. Single month ice anomaly data are far less effective in predicting conditions two or more months into the future. In these cases, typical CSI values are less than 0.5, and although the Category Error = 2 values are reasonable, the Class Error = 2 values in these cases tend to be in the range of 3 to 5, which relative to other hindcast results, is large. Finally, skill levels are moderate when attempting to employ multi-month combinations of ice anomaly data to predict one to two months ahead. In these cases (2 months July predicting August and September, 2 months August predicting September, and 3 months August predicting September), the CSI values range from 0.56 to 0.70. Again, however, the Class Error = 2 values tend to be uncomfortably large.

This exercise has been important in identifying inherent skill in antecedent ice area anomaly as a predictor of sea ice area in the Beaufort Sea region. As noted above, the best operational consequence of this fact is obtained by mating sea ice anomaly with strong meteorological predictors.

Table 4.1 Effectiveness of Antecedent Ice Area as a Predictor of Ice Area in the Beaufort Sea

Antecedent Ice Area Predictor	Employed to Predict:	"r"	"CSI"	Category Error 0	1	2	Class Error 0	1	2	3	4	Delta Rank Most Severe Cases 5	4	3	2	1
Ice area 1 month June	Ice area 1 month July	0.77	0.67	13	6	2	10	11				-3	0	-2	0	0
	Ice area 1 month August	0.49	0.49	10	8	3	7	11	3			-3	-10	-2	1	-1
	Ice area 1 month September	0.41	0.51	10	10	1	7	9	5			-9	2	-2	1	-14
Ice area 1 month July	Ice area 1 month August	0.77	0.67	15	4	2	7	14				0	-6	0	1	-1
	Ice area 1 month September	0.48	0.46	8	10	3	8	8	5			-5	2	0	1	-15
Ice area 1 month August	Ice area 1 month September	0.73	0.71	12	8	1	9	9	3			1	3	0	0	-6
Ice area 2 months July	Ice area 1 month August	0.7	0.61	11	8	2	7	12	2			0	-9	-1	1	-1
	Ice area 1 month September	0.48	0.56	12	8	1	9	7	5			-8	2	-1	1	-16
Ice area 2 months August	Ice area 1 month September	0.66	0.67	10	10	1	9	9	3			-1	3	0	0	-7
Ice area 3 months August	Ice area 1 month September	0.64	0.7	9	12		9	9	3			-2	2	0	1	-7

4.5 Effectiveness of Forecast Equations for Months Later Than Intended Issue Date

Consider a given geographical predictor domain, a particular ice predictand, and an associated issue date. Procedures described above in Chapter 2 can be executed to insolate a number of skilful multiple regression forecast equations. It would be instructive to know whether or not such equations retain any skill when used to predict ice severity in months later than the month for which the equations were initially selected. One complete example is provided here to investigate this question.

The selected region is 10 X 10 E which extends 40°N to 90°N latitude and 90° to 180°W longitude. Standard procedures were followed to generate lists of viable multiple regression equations (using meteorological predictors only) for three ice predictand/issue date combinations as follows:

Ice Predictand	Issue Date
1 month ending July	July 1
1 month ending August	August 1
1 month ending September	September 1

One sample equation, showing high skill, was then selected from each of these three combinations. The selection of these equations was based solely on skill: the presence or absence of common individual predictors in the multiple regression sets did not influence which equations were chosen to contribute to this comparison. The chosen equations were then employed to hindcast ice severity in the month for which the equation was designed, and also in all subsequent months of that same ice season, through October. The actual equations tested, and the hindcast months for each of these equations, are identified in Table 4.2. This table is a guide to the individual results which subsequently appear in Tables 4.3(a) through 4.3(c).

These latter Tables 4.3(a) through 4.3(c) present hindcast results for equations with July 1, August 1, and September 1 issue dates. The July equation (Table 4.3(a)) is employed to predict July, August, September and October conditions. Similarly, the August equation (Table 4.3(b)) predicts ice area for August, September and October, and finally the September equation (Table 4.3(c)) predicts September and October conditions only.

The nature of the results is consistent across all three months tested (Table 4.3(a) to 4.3(c)). Equations which work well in the month for which they were designed, invariably deteriorate significantly if applied in subsequent months. These equations are not stable for predicting ice conditions in later months. The deterioration in skill is evident in virtually all of the indicators, and is well characterized in the Composite Skill Index. A summary of all four cases in Figure 4.5 clearly shows that in every instance, the level of skill drops as equations are applied in months later and later than the intended issue date. This illustration suggests that it is wholly inappropriate to use equations developed for a specific ice predicand at a specific issue date, to predict ice conditions at later issue dates.

Table 4.2 Equations and Predictands Involved in Equation Effectiveness Tests
(This Table is a guide to the results prestented in Table 4.3)

Equation Employed for prediction of:	1 month July	1 month Aug	1 month Sept	1 month Oct
Equation				
Derived for use with July 1 issue date to predict 1 month July ice area: MSLP 1 June a(1) H700 5 June a(1)	Equation use as intended. Table 4.3(a) Line 1	Equation use 1 month early. Table 4.3(a) Line 2	Equation use 2 months early. Table 4.3(a) Line 3	Equation use 3 months early. Table 4.3(a) Line 4
Derived for use with August 1 issue date to predict 1 month August ice area: MSLP 7 July a(1) H500 3 July a(2) SAT 1 July a(2)		Equation use as intended. Table 4.3(b) Line 1	Equation use 1 month early. Table 4.3(b) Line 2	Equation use 2 months early. Table 4.3(b) Line 3
Derived for use with September 1 issue date to predict September 1 ice area: H1000 2 August a(1) H700 1 July a(1) SAT 1 July a(2)			Equation use as intended. Table 4.3(c) Line 1	Equation use 1 month early. Table 4.3(c) Line 2

Table 4.3 Effectiveness of Forecast Equations in Predicting Ice Area in Months Later than the Intended Issue Date

Table 4.3(a) **Use of Equations Derived for July 1 Issue Date to Predict Conditions July through October**

Multiple Regression Predictors: **MSLP 1 mos June a(1)**
H700 5 mos June a(1)

Equation Intended to predict:	Equation Employed to predict:	"r"	"CSI"	Category Error 0	1	2	Class Error 0	1	2	3	4	Delta Rank Most Severe Cases 5	4	3	2	1
Ice area 1 month July	Ice area 1 month July	0.73	0.82	13	8	0	12	2				-1	1	1	-3	0
	Ice area 1 month August	0.53	0.49	9	8	4	6	12	3			2	-15	1	1	-4
	Ice area 1 month September	0.26	0.39	6	12	3	9	7	5			-13	-1	1	1	-18
	Ice area 1 month October	0.25	0.39	10	8	3	10	6	5			-1	3	0	-18	-4

Table 4.3(b) **Use of Equations Derived for August 1 Issue Date to Predict Conditions August through October**

Multiple Regression Predictors: **MSLP 7 mos July a(1)**
H500 3 mos July a(1)
SAT 1 mos July a(2)

Equation Intended to predict:	Equation Employed to predict:	"r"	"CSI"	Category Error 0	1	2	Class Error 0	1	2	3	4	Delta Rank Most Severe Cases 5	4	3	2	1
Ice area 1 month August	Ice area 1 month August	0.77	0.85	13	8	0	8	13				1	-1	1	1	-2
	Ice area 1 month September	0.74	0.78	13	8	0	8	9	4			2	-1	1	1	-3
	Ice area 1 month October	0.53	0.61	13	8	0	9	7	5			3	-7	2	-2	-4

Table 4.3(c) **Use of Equations Derived for September 1 Issue Date to Predict Conditions September through October**

Multiple Regression Predictors: **H1000 2 mos August a(1)**
H700 1 mos July a(1)
SAT 1 mos July a(2)

Equation Intended to predict:	Equation Employed to predict:	"r"	"CSI"	Category Error 0	1	2	Class Error 0	1	2	3	4	Delta Rank Most Severe Cases 5	4	3	2	1
Ice area 1 month September	Ice area 1 month September	0.79	0.84	15	6	0	10	9	2			1	-2	1	1	-2
	Ice area 1 month October	0.58	0.60	12	8	1	10	8	3			3	-8	2	-1	-5

Figure 4.5 **Comparison of CSI Values**

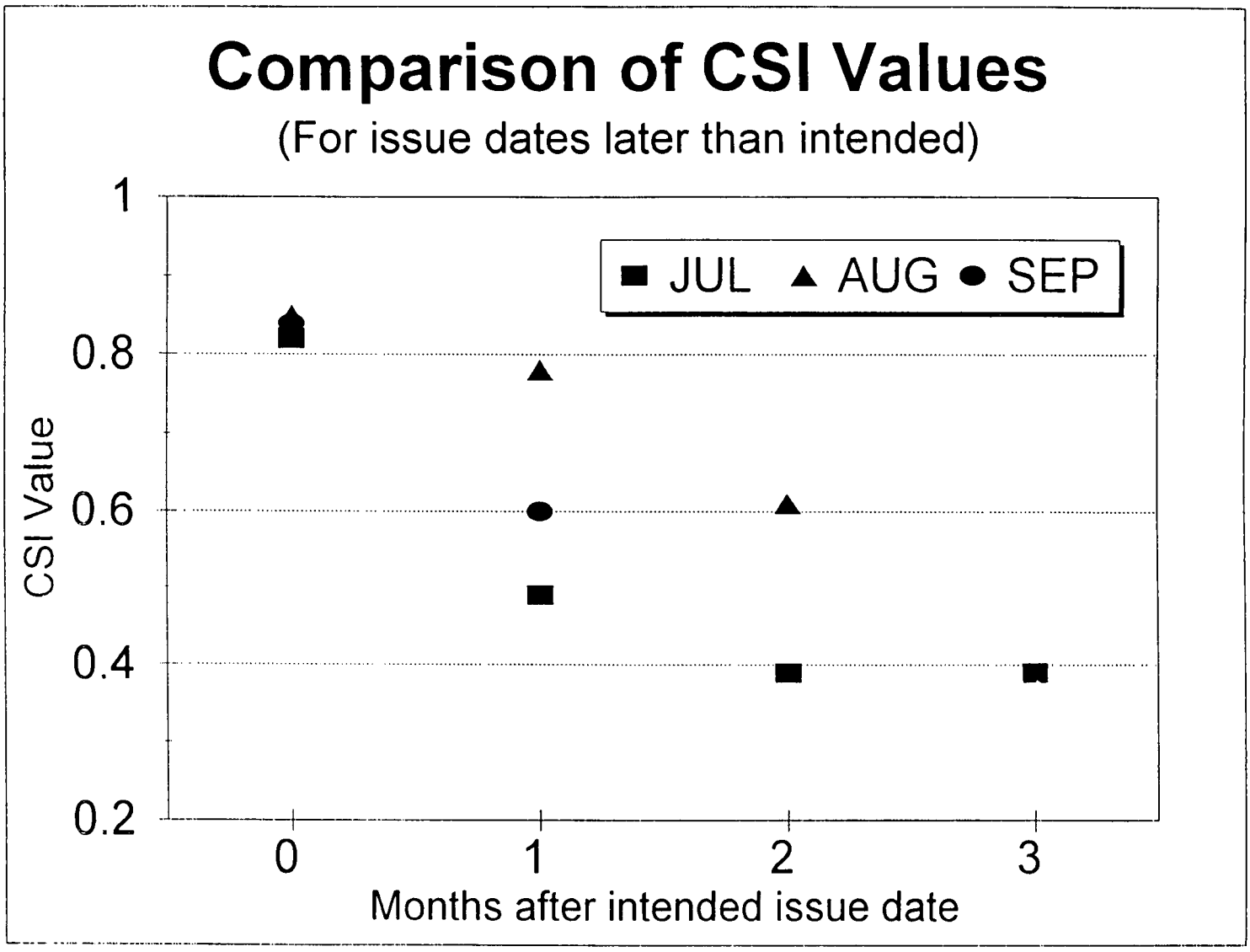

4.6 Operational Forecast Equations

Methods described in preceding chapters, including rigorous Monte Carlo tests where required (Chapter 2.5.2), have been employed in an attempt to derive viable equations for the long range prediction of sea ice area in the Beaufort Sea. Using the 10 x 10 E predictor region (Chapter 3), such attempts have been apparently successful for lead times of one month, but have been largely unsuccessful for longer lead times. Most of the equations for one month lead time, though exhibiting very high correlation coefficients and CSI values, yet contain one or more predictors which individually have long lead times or high eigenvector mode numbers, or both. Such predictors continue to lack an obvious physical explanation: nevertheless the decision has been made to retain them in the recommended equations because they have met all of the selection criteria. Particularly, they have exceeded the 95% threshold value in execution of 100 Monte Carlo simulations with random ice signal.

It is to be recalled that the multiple regression model selection process (Chapter 2.6) returns up to 50 forecast equations, ranked by high correlation coefficient and CSI values, and numbered 1 through 50. These 50 equations are derived by testing all allowable combinations of the sets of ten best individual predictors for each meteorological parameter. In the Beaufort Sea application, the number of individual predictors returned from the linear regression model tests for each meteorological parameter is typically very much less than ten, for each combination of issue date and valid time. Hence, many of the 50 multiple regression equations involve almost identical sets of individual predictors. Many such equations vary only slightly from others, due to slight differences in the number or combination of individual predictors contributing to the multiple regression model. It is after this list of up to 50 multiple regression equations is compiled that subjective judgement is required to select operational forecast equations from the list. The fact that many of the 50 equations employ very similar combinations of individual predictors allows the possibility that equations appearing far down the list of 50 might be selected for operational use, without displacing equations having much greater apparent skill.

The subjective judgements imposed in selecting the operational equations listed in this chapter for Beaufort Sea use are based on the following principles:

- consistent with east coast precedent, the decision has been taken to list up to a maximum of three equations for any combination of region/issue date/and valid date,
- up to two of these three equations are to employ meteorological predictors only,
- one of the three equations is to employ antecedent ice anomaly as a predictor,
- where possible, viable equations are sought which do not incorporate early season individual predictors, or predictors with large eigenvector mode numbers,
- where it is necessary to incorporate early season and/or high mode predictors, an attempt is made to minimize the number of these which contribute to the multiple regression model.

Applying these principles, it has been possible to compile operational forecast equation lists for the Beaufort Sea for only four circumstances, described as:

- July 1 issue date to predict one month ending July ice area
- August 1 issue date to predict one month ending August ice area
- September 1 issue date to predict one month ending September ice area
- July 1 issue date to predict three months ending September ice area.

No other combinations of issue date/valid time for the 10 x 10 E region have yielded viable forecast equations.

The selected operational equations appear in Tables 4.4(a) through 4.4(d), spanning the four cases outlined immediately above. In each case, up to three equations appear, with the last one of these incorporating an ice parameter as a predictor. Table 4.4 does not purport to rank the skill of the three equations in any group: these are simply judged to be the three best of up to 50 equations which have been returned from the automated selection process. The first column of Table 4.4 indicates the equation number from the 50 equation multiple regression list. The second and third columns provide the CSI values and the correlation coefficients. Thereafter, the individual predictors contributing to the multiple regression model are listed.

Table 4.4 Operational Forecast Equations

(a) **Issue Date:** July 1

Predictand: Ice Area One Month Ending July

#	CSI	R	Pred.	Ending	Months	Coefficient
9	0.91	0.85	MSLP	1	Jun	a(1)
			H700	5	Jun	a(1)
			D500	2	Nov	a(2)
1	0.93	0.90	MSLP	1	Jun	a(1)
			H700	5	Jun	a(1)
			D500	1	Nov	a(2)
			ICEA	1	Jun	

(b) **Issue Date:** August 1

Predictand: Ice Area One Month Ending August

#	CSI	R	Pred.	Ending	Months	Coefficient
1	0.98	0.96	SAT	4	Feb	a(4)
			H1000	4	Feb	a(4)
			H700	5	Jul	a(1)
			D500	2	Nov	a(2)
22	0.97	0.95	SAT	1	Nov	a(5)
			MSLP	5	Jan	a(5)
			H700	1	Jul	a(1)
			D500	3	Jul	a(1)
2	0.98	0.96	SAT	4	Feb	a(4)
			H1000	4	Feb	a(4)
			H700	5	Jul	a(1)
			D500	2	Nov	a(2)
			ICEA	1	Jul	

Table 4.4 (cont.)

(c) **Issue Date:** September 1

Predictand: Ice Area One Month Ending September

#	CSI	R	Pred.	Ending	Months	Coefficient
1	0.94	0.93	SAT	1	Aug	a(4)
			MSLP	6	Aug	a(1)
			H500	5	Feb	a(3)
			D700	2	Jul	a(5)
4	0.93	0.89	SAT	1	Jul	a(1)
			H1000	3	Jan	a(2)
			H700	1	Jul	a(1)
			D700	2	Jul	a(5)
35	0.92	0.88	SAT	1	Aug	a(4)
			H1000	2	Aug	a(1)
			D700	2	Jul	a(5)
			ICEA	1	Aug	

(d) **Issue Date:** July 1

Predictand: Ice Area Three Months Ending September

#	CSI	R	Pred.	Ending	Months	Coefficient
5	0.92	0.88	MSLP	6	Jun	a(1)
			H500	3	Jan	a(3)
			D500	2	Nov	a(2)
1	0.93	0.92	MSLP	6	Jun	a(1)
			H500	3	Jan	a(3)
			D500	2	Nov	a(2)
			ICEA	1	Jun	

5. CONCLUSIONS AND RECOMMENDATIONS

The objectives of this work, as first presented in Chapter 1.3, can be simply reiterated as:

- to generalize LRIFS for use with hemispheric predictor files,
- to prepare hemispheric predictor data files,
- to prepare Beaufort Sea ice area data in the form of predictand time series, usable by LRIFS,
- to automate the execution of simple and multiple regression tests,
- to develop operational forecast equations for predicting Beaufort Sea ice area severity, and
- to report findings to ESRF and Ice Centre Environment Canada.

The work which has been completed, as reported in Chapters 2 through 4 of this document, has met or exceeded each of these specific objectives. It remains the role and purpose of this concluding chapter to discuss the findings and evolution of this work, both from the perspective of a direct application of LRIFS for Beaufort Sea use, and from the broader perspective of LRIFS as a research tool for ice prediction in Canadian waters.

Considering first the broad perspective, it is certain that this work has yielded structural changes which represent significant improvements to LRIFS as a research tool. The generalization of predictor fields to span the northern hemisphere, the organization of nearly 40 years of predictor data on the hemispheric grid for seven meteorological parameters, the introduction of the Cumulative Skill Index (CSI), the automation of linear and multiple regression model procedures, the unanticipated introduction of the Monte Carlo screening process, and the total rebuilding of the LRIFS user interface are all significant contributions. Each of these accomplishments contributes to the future utility of LRIFS. Coupled with this technical report, the System Specification and Users Manual documents (Pinhorn, 1993a and Pinhorn, 1993b) which were completed as part of this work, are the records of such accomplishments.

The work has been less successful in its goal to provide an operational forecast system for use in the Beaufort Sea. The fact that no prediction equations with lead times greater than one month have been identified is a unexpected disappointment, after similar approaches have offered longer lead times, especially for icebergs, on the east coast. Even the equations which have been selected (Chapter 4.6) continue to be plagued by one or more unusual predictors having individual lead times of many months and/or having high eigenvector mode number. These equations have been retained because they meet the conditions presently established for LRIFS equation extraction; however, their long term utility remains somewhat questionable.

There are three specific research/development activities which are immediately recommended as a means of improving confidence in the Beaufort Sea equations. These recommendations, and the rationale for each, are individually described.

Firstly, it should be recognized that the 1960 to 1980 interval over which AES digital sea ice data are available for the Beaufort Sea is statistically very short. The single most important action which should be taken to improve LRIFS for Beaufort Sea operation is to digitize the

relevant sea ice data for the years 1981 through 1992, thereby extending the predictand time series by more than 50% in duration. This action should better define the real variability which these hindcast models seek to reproduce, and should result in the derivation of more stable predictive equations, if such exist. Extension of the predictand interval should also have the desired effect of reducing the incidence of artificial skill in predictors.

Secondly, further investigations with the Monte Carlo model are advised, as a means of further probing the long lead time and high mode predictors. At least the following two tests could be useful:

- increase the number of random tests from 100 to 200 or more, to determine whether these unusual predictors still pass the Monte Carlo tests, and

- increase the threshold value from 95% to possibly 98%, to determine whether or not this change alters the number of predictors which pass the Monte Carlo test.

Finally, attention could be redirected to the choice of the geographical domain for predictor selection. Results presented in Chapter 3 showed only slight variations in skill for equations derived from regions 7 x 7, 8 x 8, 9 x 9, 10 x 10 E, and 11 x 11. The region 10 x 10 E was employed in deriving the operational equations which are tabulated in Chapter 4.6. It is recommended that the entire equation extraction process be repeated, using the small 7 x 7 predictor region, and that the results of this work be carefully compared with the 10 x 10 E results included in Chapter 4.6 of this report, to further search for defensible, stable, Beaufort Sea forecast equations.

REFERENCES

Barnett, D.G., 1980. "A Long-Range Ice Forecasting Method for the North Coast of Alaska" Sea Ice Processes and Models, R. S. Pritchard, Ed., Univ. of Washington Press, pp. 360-372.

Chapman, W.L., and J.E. Walsh, 1991. "Long-Range Prediction of Regional Sea Ice Anomalies in the Arctic" Weather and Forecasting, Vol. 6, No. 2, pp. 271-288.

Davidson, L.W., 1992. "Long Range Ice Forecasting System (LRIFS) Technical Report". Report prepared for Atmospheric Environment Service, Ice Centre Environment Canada (ICEC), Ottawa.

Davidson, L.W., 1987. Advances in Long-Range Prediction of Grand Banks Iceberg Season Severity. Report prepared for Atmospheric Environment Service, Ice Centre Environment Canada (ICEC), Ottawa.

Davidson, L.W., W.I. Wittmann, L.H. Hester, W.S. Dehn, J.E. Walsh and E.M. Reimer, 1986. "Long-Range Prediction of Grand Banks Iceberg Season Severity: A Statistical Approach." Environmental Studies Revolving Funds, Report No. 048, Ottawa.

Davis, R.E., 1976. "Predictability of Sea Ssurface Temperature and Sea Level Pressure Anomalies Over the North Pacific Ocean." J. Phys. Oceanog. Vol. 6, No. 3, May 1976.

Hibler, W.D. III and J.E. Walsh, 1982. "On Modeling Seasonal and Interannual Fluctuations of Arctic Sea Ice" J. Phys. Oceanogr., Vol. 12, pp. 1514-1523.

Johnson, C.M., P. Lemke, and T.P. Barnett, 1985. "Linear Prediction of Sea Ice Anomalies" J. Geophys. Res. Vol. 90, No. D3, pp. 5665-5675.

Marko, J.R., D.B. Fissel and J.R. Birch, 1986. "Physical Approaches to Iceberg Severity Prediction". Environmental Studies Revolving Funds Report No. 038, Ottawa.

Mysak, L.A., and D.K. Manak, "Arctic Sea-Ice Extent and Anomalies, 1953-1984", Atmosphere-Ocean, 27(2), pp. 376-405.

Neville, A.M and J.B. Kennedy, 1966. "Basic Statistical Methods for Engineers and Scientists." International Textbook Company, Scranton, PA.

Pinhorn, J.B., 1993a. "The Long-Range Ice Forecasting System (LRIFS) System Design and Maintenance Document, Version 3.0." Report prepared for Atmospheric Environment Service, Ice Centre Environment Canada (ICEC), Ottawa.

Pinhorn, J.B., 1993b. "The Long-Range Ice Forecasting System (LRIFS) User Manual, Version 3.0." Report prepared for Atmospheric Environment Service, Ice Centre Environment Canada (ICEC), Ottawa.

Walsh, J.E., 1980. "Empirical Orthogonal Functions and the Statistical Predictability of Sea Ice Extent" Sea Ice Processes and Models, R. S. Pritchard, Ed., Univ. of Washington Press, pp. 373-384.

Walsh, J.E. and J.E. Sater, 1981. "Monthly and Seasonal Variability in the Ocean-Ice-Atmosphere System of the North Pacific and the North Atlantic." J. Gephys. Res., 86(C8), pp. 7425-7445.

APPENDIX I Derivation of Empirical Orthogonal Functions

The essential features and merits of empirical orthogonal functions are well described by Walsh and Sater (1981). Discussing the large volumes of sea level pressure (SLP) and sea surface temperature (SST) data which they had prepared for use in studying sea ice/atmosphere interactions, these authors note that,

"In view of the large volume of SLP and SST data, much of the analysis and discussion is based on the dominant patterns of variability of the data fields. These patterns are empirical orthogonal functions (EOF's), which are also referred to as eigenvectors or principal components. The first eigenvector of a set of data fields is the dominant mode of variability in the sense that it describes a greater percentage of the variance of the data fields than does any other pattern. Each succeeding eigenvector describes a maximum of the variance that is unexplained by the previous eigenvectors. The coefficient or amplitude of an eigenvector is a measure of the extent to which that eigenvector pattern is present in a particular anomaly field.

Among the advantages of the eigenvector representation are the effective compression of the data and the orthogonality (independence) of the patterns in space and time."

Derivation of Empirical Orthogonal Functions

It is desired to calculate the characteristic functions of a set of atmospheric data such as the mean sea level pressure, 500 mb or 700 mb height, 500 mb - 1000 mb or 700 mb - 1000 mb thickness, surface air temperature, or some other parameter. Suppose that the data are symmetrically organized on a geographical latitude/longitude grid, and that data values at each grid point are available over some routinely spaced series of times. Such values can be considered as a regular time-series of (spatially varying) data fields. Let the data values for points of fixed latitude define the rows of a matrix and similarly let the data values for points of fixed longitude define the columns of this same matrix. One such matrix (or grid) exists for each time.

By summing such matrices for a selected number of times and dividing by the appropriate number of cases it is a simple matter to compute the time averaged or mean representation of these fields. Then by subtracting this mean from the measured fields, it is possible to compute anomaly fields.

Such zero-mean anomaly fields (for any selected scalar parameter) can be represented as:

$$P = P(x,y,t)$$

where $x = x_1, x_2 \ldots x_{N1}$ N1 = number of columns (longitude)

$y = y_1, y_2 \ldots y_{N2}$ N2 = number of rows (latitude)

$t = t_1, t_2 \ldots t_M$ M = number of time intervals

Combining the two spatial dimensions into one spatial parameter $\underline{x}$, the field can be represented as:

$$P = P(\underline{x},t)$$

where $\underline{x} = \underline{x}_1, \underline{x}_2 \ldots \underline{x}_{N1\,N2}$

Following the arguments of Davis (1976), the time averaged correlation matrix of the anomaly fields can be computed as follows:

$$R_{ij} = \frac{1}{M} \sum_{k=1}^{M} P(\underline{x}_i,t_k)\, P(\underline{x}_j,t_k)$$

The matrix R_{ij} is dimensioned $N_1N_2 \times N_1N_2$.

The eigenvectors $E_n(\underline{x})$ of R_{ij} are the empirical orthogonal functions of the data fields: the associated eigenvalues λ_n describe the contribution of each eigenvector to the total variance in the data fields. Those $E_n(\underline{x})$ with the largest λ_n are the principal modes of the data fields.

While there exist N_1N_2 eigenvectors, it is usually true that a small number of these describe a large percentage of the variance in the signal. To what extent this is true can be determined by examining the parameter λ'_T defined as:

$$\lambda'_T = \sum_{n=1}^{m} \lambda'_n \quad \text{for } m << N_1N_2$$

(The primed quantities simply denote normalized values.)

As λ'_T approaches 1.0, the number of important eigenvectors (m) can be determined.

It is thus possible to reconstruct any of the observed fields $P(\underline{x},t)$ as a superposition of $E_n(\underline{x})$. Formally,

$$P(\underline{x},t) = \sum_{n=1}^{m} a_n(t)E_n(\underline{x})$$

Using the dot product operator, it is possible to determine the $a_n(t)$ as:

$$a_n(t) = P(\underline{x},t) \bullet E_n(\underline{x}) \qquad n=1,\ m$$

The net result is a reduction of M grid patterns of observed data of dimension N_1N_2, to m time-series of scalar coefficients $a_n(t)$, with $m << N_1N_2$, and typically less than ten. These $a_n(t)$ are the "coefficients or amplitudes" of the eigenvectors, as described by Walsh and Sater (1981). They describe the extent to which the particular eigenvector is present in any particular measured anomaly field.

This publication is printed on paper containing recovered waste.